The Investigation of Grain Boundary Development and Crystal Synthesis of Thin Gold Films on Silicon Wafers.

Gavin Stenning

Supervisor: Ian Robinson
Second supervisor: Neal Skipper

Degree: MSci Physics

31/03/09

Abstract

To investigate the stages that lead up to gold crystal synthesis and the conditions under which these processes occur, in particular the formation of grain boundaries in thin gold films. This is achieved through annealing of films to set temperature and analysis under scanning electron microscope.

Crystal synthesis from thin films starts with hole formation then break up (675-725˚C) for gold-chromium and (250-400°C) for gold-titanium and progress to gold crystals. Chromium acts as an adhesion layer where titanium acts as a lubrication increasing rate of dewetting to crystal synthesis.

Contents

Acknowledgements

Ian Robinson, Neal Skipper, Moyu Watari, Steven Leake, Marcus Newton, Loren Bietra, khashayar Ghaffarzadeh, Kevin Reeves (Institute of Archeology).

Chapter 1

Introduction

At present the dewetting of a gold film onto a silicon wafer is not a uniform process, even though the sample is exposed to the same temperature and gases. When the sample is removed from the equipment it contains unknown phenomena, this has yet to be explained.

This study into the dewetting of gold films to produce randomly-orientated crystal grains is essential to understanding their structure. There is a need for uniform silicon wafers of gold crystals to be produced so coherent X-ray diffraction experiments can take place. This will enable clear images of their diffraction pattern to be obtained before the sample is destroyed by the radiation exposure. The dewetting of the gold film to the crystal stage requires investigation enabling multiple samples to be created successfully.

Aim

The aim of this project is to investigate the stages that lead up to gold crystal synthesis and the conditions under which these processes occur. In particular the start of the grain boundary formation on the surface of the gold film (grooving) and the consecutive steps that follow. Proceeding to the separation of the “rivers” (linear array of grains whose interface energies keep them together) then crystallise into randomly-orientated crystals on the silicon wafer surface.

The investigation will also look into why some grains have inhomogeneous coarsening. In these cases there appears to be a large quantity of the gold film with no visible grain boundaries or in which no changes have occurred during experimentation when it is all expected to occur at the crystal stage.

Dewetting gold

The dewetting of gold to produce randomly orientated crystals is to provide a sample by which coherent X-ray diffraction can take place. It will then give an accurate image for the crystal structure. The using of gold films as the randomly orientated crystal is because

the processes that lead up to the fully dewetted crystals is still relatively unknown. The temperature at which the crystals are fully dewetted and all the grain boundaries have broken up is not known, this is the same story throughout the whole dewetting process of the gold film.

The use of gold film rather than any other metal is because gold is a relatively inert metal therefore will not react during the annealing heat treatment process. It is important as the temperature required to completely dewet the gold film is approaching the melting point of gold (1064˚C [31]) which at these temperatures if an inert metal is not used then oxides and other reactions may react with the gold.
The gold films that are used have a thickness of 20nm. The thickness of the gold film has been chosen such that it is the most optimum thickness for the experiments taking place. If the thickness of the film were to be greater than 20nm (≈200nm for previous experiments) then because the dewetting process is dependent on both the temperature that the sample is subjected to and the time that this temperature is applied, then for a thicker gold film the time required to fully dewet the film will be much longer then a thinner film. The alternative would be to increase the temperature for the same time length, but this is a more inaccurate method as the temperature necessary would be that approaching the melting point. For a film thickness of less then 20nm then there is the possibility that during the annealing process the gold film may evaporate, leaving the crystals completely evaporated or much reduced then first anticipated. At this thickness the annealing time would be excessive leading to problems with the adhesion layer and its diffusivities.

Coherent X-Ray Diffraction

Coherent X-ray diffraction is the experimental procedure that gives the image of the crystal structure. Coherent X-rays are Bragg diffracted from the gold crystals on the sample surface. The X-ray beam that is used to illuminate the sample surface has a specific spot size, as therefore as the beam moves over the sample there are overlapping of simultaneous diffraction patterns.

What information this gives is a phase change in the diffraction pattern, therefore it is this phase change that carriers all of the virtual information of the crystal structure. The phase change that occurs cannot be physically measured and so there are a number of ways which the phase information can then be reinterpreted this is known as a phase problem and the current solution to this problem are two algorithms known as the Hybrid input output and the Error reduction methods. Both of these algorithms use approximately 50-100 iterations. With each new iteration a new piece of physics is implemented to give further detail to the real space image.

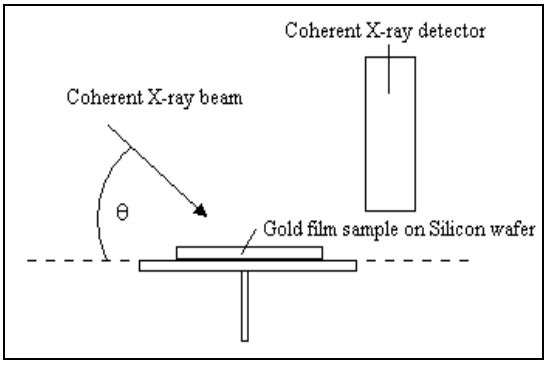

Figure 1: The experimental procedure for coherent X-ray diffraction.

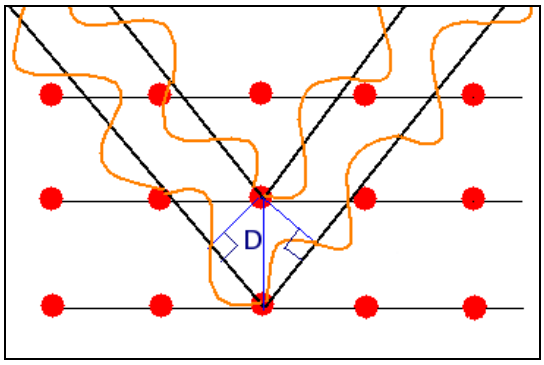

Figure 2: The X-Ray Bragg diffraction at the sample surface

Figure 1 shows the experimental set up of how the X-ray diffraction takes place, and figure 2 shows the physics of the Bragg diffraction at the crystal scale. The angle θ that is shown in figure 1 is the angle which the coherent X-ray makes with the surface of the illuminated sample, this angle is dependent on the area of the sample of which is needed to be studied, Its maximum value is 5˚ and this would hit an area of approximately one crystal therefore a shallower angle to have a Bragg diffraction from a larger area (more than one crystal) would be approximately 0.1˚.

Figure 2 shows how the coherent X-rays are diffracted from the sample through use of the Bragg equation. It can also be seen that as the wavelength of the coherent X-rays is sufficiently small it can penetrate further into the sample before being diffracted.

$$N\lambda = 2d \sin \theta$$

λ=Wavelength

D=Distance between crystal planes

θ =Angle of diffraction

The phase is the most important information that can be retrieved as it can recreate the real space image whereas the amplitude cannot, a superposition of both phase and amplitude gives a reconstruction of the real space image at a much better resolution.

The free electron laser which is used for this process has outstanding consideration concerning its use that once the diffraction pattern has been obtained the free electron laser destroys the sample. This is due to the free electron laser being a high power pulsed laser. The implication of this is that in order to have randomly orientated crystals for the diffraction experiments first the method of producing the crystals must be understood.

Reproducible Samples and Irregularities

The need for the gold films on the silicon wafer to be reproducible is due to the free electron laser destroying the samples from which it obtains any images. This means only one real space image can be taken from each sample. The need for many uniform samples of randomly orientated crystals is essential. The process of obtaining these samples is not fully comprehended. This means that when the coherent X-ray diffraction experiments take place because there is inconclusive information about the formation of the crystals there are some irregularities in the sample diffraction pattern.

The irregularities occurring during the dewetting stage of the formation of the sample is when the grains should all break up or coalescence into larger crystals.

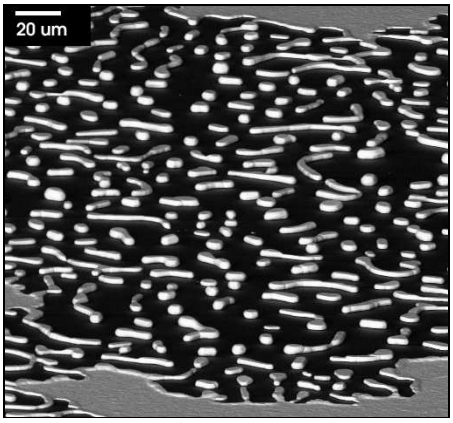

Figure 3: SEM image of 1000Å gold film after dewetting stage [1].

Figure 3 shows a gold film after the dewetting stage. It is shown there is a number of irregularities as this SEM image should only contain the uniform randomly orientated crystals. In the image there are areas where there are still several grains in long chains still yet to break up “rivers” (groups of undissociated grains). There are also large areas of gold film visible where there has been no apparent change or even the starting of the grain boundary formation. The last ambiguity from the image is that around the edges of the larger areas of un-dewetted gold film (plates) there appears to be a raised lip around the edge of the plates. These irregularities and reasoning behind why only some of the gold film has fully dewetted and the plates seem relatively untouched is not fully understood. On introspection proceedings assume to be developing the dewetting stage. The inhomogeneity of the gold film can be said to have an increase in the films polydispersity.

When the thin film is partially dewetted so that part of the sample is in crystal formation and other regions plate format, there can be observed that a lip around the edge of the plate may be seen as in figure 3. The nature of this lip on the formed island can be due to one of two possibilities, either a process of the dewetting where the edge grain coarsens to a larger size before the grain boundary forming through to the substrate before separation, or oxygen diffuses around the edge of the island to the SiO_2 underneath. This would then cause the SiO_2 to grow in thickness therefore rising up the gold layer thereby giving the appearance of the island lip.

There are other structures found at random throughout the sample, these are such as Holes. These are found on the sample and are where there is a hole in the gold film and in the silicon dioxide all the way through to the silicon wafer. This seems to prohibit any gold evaporation on this area of the sample or for much easier gold break-up. The implication of holes being present on the sample surface does not seem to have a large effect on present results. It can be expected that as the hole penetrates through to the silicon wafer then the dewetting of the gold film may start at the edges of the structure this would be due to the gold grains at the edge having a larger surface area open to the effective temperature then that of the uniform flat film.

There are also some irregularities that stand up approximately 500Å from the original surface level of the film, it is thought that the change may have arisen due to thermal shock or from thermal expansion.

Gold Film Irregularities and Plausible Solutions

The most likely solution to these irregularities that can be seen on the gold film is that of contamination from the ambient air and dust particles. Although the evaporation and the annealing of the sample will take place in a class 100 cleanroom the samples need to be taken through normal air (in a clean container) to the SEM equipment, so at each experimental stage there is risk of contamination. The solution to this problem is to keep the samples stored in nitrogen filled bags for the duration between stages of the experiment thereby limiting the time exposed to any other gas apart from nitrogen.

The differences between the stages of the dewetting of the gold film may also have the basis that there may be a variation in the thickness of the gold film thereby leading to different rates the dewetting occurs at. The way to solve this issue is to create the samples that are to be used to a known thickness of gold that is deposited and to have as much of the process automated as possible.
Free volume regions within the gold film may lead to ambiguities on the films surface due to thermal expansion of the free region leading to a surface film distortion [2].

As the film and the substrate are both reaching temperatures in order of ~600˚C+ then there can be some expected thermal expansion of the silicon wafer as well as the gold film sample. The thermal expansion of the two materials could cause a compressive or tensile force dependent on which material has the greatest thermal expansion coefficient. The thermal expansion coefficients are as shown below:-

$$\text{Au} = 14.2\mu\text{m m}^{-1}\text{K}^{-1}$$
$$\text{Cr} = 4.9\mu\text{m m}^{-1}\text{K}^{-1} \quad [31]$$
$$\text{Si} = 2.6\mu\text{m m}^{-1}\text{K}^{-1}$$

Thermal Expansion Tables

650 °C			650 °C		
	Δ Temperature(K) = 6.25E+02 Original length(mm)	Δ Length (nm)		Δ Temperature(K) = 6.25E+02 Original Thickness (nm)	Δ Thickness (nm)
Au	0.01	8.75E-05	Au	2.00E-08	1.75E-10
Cr	0.01	3.06E-05	Cr	2.00E-09	6.13E-12
Si	0.01	1.63E-05	Si	1.00E-03	1.63E-06

Table 1: Changes in sample length and thickness due to thermal expansion of samples during annealing process.

The above table using the linear thermal expansion coefficients shows an example of the change in the relative lengths and thickness of a sample 1cm in length and 20nm in thickness. They show that the gold film has the greatest expansion of the materials present, with the silicon wafer having the least. This may result in the gold film expanding in areas and compressing in others, forcing some gold grains above the surface of the film forming “hills” [3].

There is a similar trend when taking into account the volumetric thermal expansion of the three materials. Table 1 are calculated at a temperature of 650°C, this was calculated as was the most common temperature for annealing procedures and so was therefore the most useful.

The thermal expansion of the sample was considered for further calculations of the percentage of gold coverage of the SEM image of the sample and as to its effect.

Previous Experiments

There have been a number of previous experiments which have investigated other aspects of the grain boundaries.

The most relevant of which investigated the diffusion effects in films of gold on chromium [4]. A borosilicate glass substrate was used with 10nm of chromium and 400nm of gold evaporated onto the surface of the substrate. The substrate showed some certain diffusion effects occur at the grain boundaries. The effects were the gradual emergence of ridges of the materials decorating the grain boundaries and a change in the surface profile in which the crystallites stand out as islands. The production of the sample was first an evaporation process of the metals, then annealing the samples at 300°C for a total of 11 hours.

The annealing process was separated into three sessions, the advantage of which the grain boundaries may be examined at each intermediate stage. This is achieved by at each stage a collodion carbon replica of a selected area of the surface was examined using an electron microscope.

The results that were obtained from this experiment showed that after annealing at 300°C for three hours ridges appeared in the surface indicating the positions of grain boundaries. The following two annealing sessions of the samples were for two and six hours successively.

After the final annealing run the gold film was then removed leaving the chromium underlayer. It can be seen that the remaining chromium layer had migrated into an inhomogeneous pattern, which ultimately followed the same area and size of that as the gold crystallites.

This result is evidence that the chromium adhesion layer has begun to diffuse through the gold grain boundaries. The implication of the chromium diffusing through the grain boundaries is that once diffused to the surface the chromium will form Cr_2O_3 [5] upon exposure to air [6]. For longer annealing times the diffusion of the chromium layer leads to a complete depletion of the continuous adhesion layer, therefore creating a near uniform through thickness gold-chromium material. This would occur for a long time periods of annealing time [7].

Other previous experiments have again shown the polydispersity of the thin film with no reason for this ambiguity. The conditions for the SEM image collected (Figure 3) was annealing a gold film of thickness of 100nm for duration of 18 hours at 1225˚C yielding randomly orientated crystals alongside rivers and isolated island of gold[1].

Chapter 2

Theory

Grain Boundary Formation

The purpose of this project is to investigate the initial stages of the grain boundary formation of the thin gold film to crystal synthesis. There are a number of processes that occur at the grain boundary and during the annealing process. The processes include, grain boundary kinematics, the coalescence of the grains, the diffusion of the adhesion layer between grains and grain boundary motion [8].

To comprehend the processes that occur in the gold film at the grain boundary, firstly the sample as a whole needs to be inspected. The annealing process will take the gold film close to the melting point of gold, therefore the material which the gold film is placed on needs to be able to withstand high temperatures.

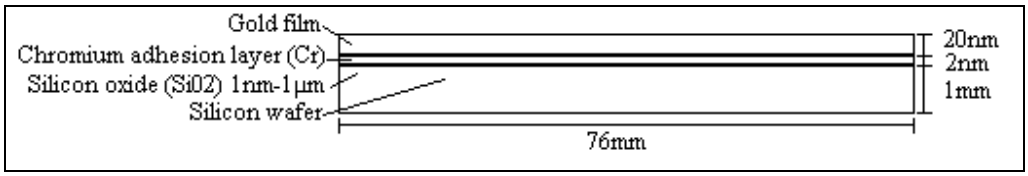

Figure 4: Diagram showing the composition of the sample which will be created and then annealed.

Figure 4 shows the composition of the sample that will be created for the purposes of this project. It shows that the substrate base on which the gold will be evaporated onto to be a silicon wafer as this will be capable of withstanding able to withstand such high temperatures much over 1000°C without any deformation or softening. The figure also shows two other layers which are of great importance, the silicon oxide layer and the chromium adhesion layer.

The silicon oxide layer (SiO_2) occurs naturally on the silicon substrate and occurs through oxidation of the silicon crystal structure.

The adhesion layer is an essential part of the composition of the sample. The object of the chromium adhesion layer is that gold as an inert metal and does not easily form bonds or react with the surface of the silicon surface, so in effect the adhesion layer bonds to the surface of the silicon wafer and then each material's oxides diffuse into each other forming the bonds.

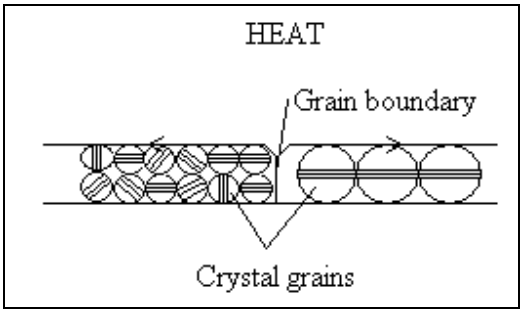

Figure 5: This shows the starting of the grain boundary formation and how the grain orientation changes.

Figure 5 shows how the grain boundary formation occurs in respect to the gold grain orientation. Figure 5 on the left side of the image indicates how the grains at the start of the annealing process are completely random and are small, as the annealing process continues the grains will coalesce and coarsen into larger grains and the orientation changes so that all of the grains will become aligned. The alignment and coalesce of the gold grains are shown on the right side of figure 5. The grains will also coalesce to the thickness of the film even during the evaporation process or at very low annealing temperature. The study of the unannealed samples shows the average grain size to be ~20nm in size. The final crystal size is, on average 200nm in length so the grains seem to grow in size by a factor of 10 by two main processes, coarsening and coalescence.

Coarsening of Grains

This is the process by which the average island size within a system of isolated islands can increase through detachment and diffusion of atoms on substrate surface to other isolated islands, even if the deposition is interrupted [9]. This leads to an average increase in the gold plate size, as the smaller structured plates disappear through this effect.

The diffusion of atoms from one part of the sample to another is driven by differences in the energy of each atom which diffuses to a different location [10].

Coalescence of grains

Density and size of crystallites were found to increase with an increase in the annealing temperature. This is the process whereby two islands have grown to the point of contact.
When two grains come into contact with one another there exerts a driving force for the formation of a grain boundary, this formation of the grain boundary then eliminates the energies of the free surfaces of the two contacting grains, in exchange for a lower energy of the grain boundary [10].
This is the process by which when grains come into contact there can be some migration of an atom or a group of atoms from one grain to its neighbour across the grain boundary.
In a one dimensional system the velocity of the interface by atoms is given by:-

$$V = rA\mu(\Delta\mu/KT)\exp(-\Delta g/KT) \qquad [11]$$

Where r is the distance moved per activated event, A is a geometric factor, $\Delta\mu$ the chemical potential change driving the process, Δg the free energy of activation which is usually associated with grain boundary diffusion, with K being Boltzmann's constant and T temperature [10].

Grain Boundary Kinematics

Grain coarsening occurs through the motion of grain boundaries resulting in the disappearance of smaller grains and therefore increasing the remaining grain size. This process is known as grain growth. Grain growth and grooving are competing kinematic processes. This leads to the approximation that grooves will not form on rapidly moving boundaries. As the velocity of the boundary decreases the grain boundary grooving will start to form and so reduce and then prohibit further boundary motion [12].
The two interfaces of the film and their associated energies also affect the grain growth in thin films. The energies of the surface of the film and of the film/substrate interface are both affected by the crystallographic orientations of the grains [10].

The result of this is that there will be some orientation of the grains which will yield a minimum surface energy. The orientations of these grains to there effective ground state is also not necessarily the same orientation throughout the entire sample. It is shown in figure 6. There can also exist some alignment of the grains relative to one another so as to minimise the sum over all energies.

The grain boundary curvature relative to the normal may then be seen taking into account of the surface and interface energies to be giving:-

$$\Gamma = (\Delta\gamma_s + \Delta\gamma_i) / \gamma_{gb}h \qquad [10]$$

Where Γ is the out of plane curvature of the grain boundary, $\Delta\gamma_s$ and $\Delta\gamma_i$ are the change in the surface and interface energies at the grain boundary under investigation, γ_{gb} is the grain boundary energy and h the film thickness.

The effects and magnitude of the surface and interface energies become more apparent in thinner films [28].

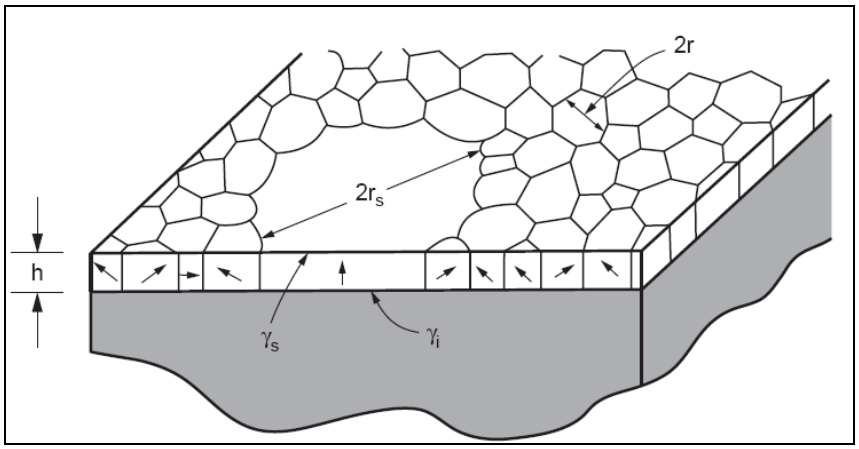

Figure 6: The Grain evolution of thin metal films on silicon substrate [10].
Showing surface energy γ_s and interface energy γ_i.

Groove Evolution

When the film reaches a significant temperature to allow for atomic migration a thermal groove will develop along the line where a grain boundary intersects the surface [11].

The Groove that appears on the film surface may develop through several processes such as evaporation, surface and volume diffusion and annealing of the sample.

The groove profile at its root can be controlled by the equation:

$$\tan^{-1}(\gamma_{gb}/2\gamma_s) \qquad [13]$$

Where γ_{gb} is the grain boundary and γ_s is the surface energy. The groove can then develop by surface diffusion mechanisms for small grooves [14] by which the depth of the groove increases by $(\text{time})^{1/4}$. This grooving of the thin films is what limits the stability of the film [13].
The groove angle increases with time and also the speed of which the grooving occurs increases with the groove depth.

The groove which forms in the thin film is also dependent upon the purity of the material for during the evaporation procedure. The effect that impurities have upon the groove formation is that when the atomic radius of the impurity is smaller then that of the gold and gold/impurity bond energy is close to the gold/gold bond energy, groove formation is prevented due to the suppression of the diffusion [15].

Gold is a face centred cubic structure has a low stacking fault energy which indicates that gold films favour grain boundary dissociation [16].

Rate of Evaporation

During deposition of the gold if the film is deposited fast approximately 30Å/S exhibits grain boundary diffusion which can be observed [17].
Whereas with films that are deposited at a slower rate, 3Å/S underwent catastrophic change in their structure and shows very little if any grain boundary diffusion.

For the purposes of this project the rate that is going to be used is approximately 1Å/S for the adhesion and 0.4Å/S for the gold layer, reasoning being that it is the lowest rate that the equipment can successfully go to, this means there will be some grain boundary diffusion but this should be minimised. Thereby limiting the grain growth before the annealing process occurs.

One reason for using silicon as the substrate for evaporation of the metal films is due to it being atomically flat. This is a benefit as the dewetting rate also decreases with an increase in the substrate roughness. The atomically flat substrate can be seen occasionally after annealing processes when the gold may form squares where it has "sunk" into the substrate (SiO_2) hence taking its crystal shape

Silicon Wafer / Silicon Dioxide Orientations and Crystal Structure

The silicon wafer is comprised of two parts. The silicon wafer crystal and the silicon dioxide that resides on the surface.

On inspection the silicon wafer one side appears to have a metallic finish and the other a "matt" finish. This is due to the silicon dioxide having a (111) crystal orientation and the silicon (100). The crystal structure of silicon is diamond cubic. The silicon dioxide is more complicated as there are various forms. The structure consists of the oxygen atoms bonded in between two silicon atoms, however silicon dioxide is not a diamond cubic like silicon it is an amorphous structure. It is not a uniform structure and there are bonds missing but of magnitude of less then a few percent. The differences arise as the bonding between each silica atom and four identical oxygen atoms throughout the structure but the Si-O-Si inter tetrahedral angle can form torsional angles. The rotation and bending of this bond then give the structure its amorphous structure and can then be seen using a radial distribution function. The structure does not have long range order as the function produces a damped oscillation. A long range ordered structure such as a silicon crystal would have a radial distribution function that is sinusoidal. The silicon dioxide can be natural or induced. The oxygen diffuses through the SiO_2 to the crystal interface where it bonds with the silica therefore growing. The natural oxide is a spontaneous reaction with the bare silicon being saturated with hydrogen and the O_2 growing on the surface, this process yields approximately 2-3nm in thickness. The induced growth of silicon dioxide is when the silicon is heated to temperatures in excess of 850°C in an oven with O_2 present. This method can give much greater thicknesses typically over a micron.

The samples made will experience temperatures of anything up to 1000°C, the implications this has on the silicon dioxide at this and lower temperatures is that silicon dioxide will start to soften and therefore become increasingly random in its structure. For

the gold this means that as the SiO_2 softens then the gold crystals sink into the SiO_2 [18], however the majority of the crystal is above the interface plane. The adhesion layer has very little or no effect at this stage as the wetting layer is depleted. A secondary effect that occurs from the annealing process is that as the gold grains break up the SiO_2 can then be grown as the temperature is approximately the same as in growth conditions, this can lead to SiO_2 diffusing/growing between the gold grains. The growth of the SiO_2 is approximately above 850°C and is also thought that the growth of this layer is when oxygen diffuses through the layer to the crystal interface whereupon contact with the silicon forms its oxide [19].

This process can also take place at the edge of isolated regions of gold where the O_2 would diffuse under the film so therefore the SiO_2 can increase in thickness under the gold leading to a raise in the gold film above the plane.

Adhesion Layer

The adhesion layer is a thin film of metal about 1-5nm thick and can be found at the interface between the silicon oxide and the gold film.

The two purposes why it is necessary to bond the two together is [6], due to gold being a very inert metal so the adhesion is necessary otherwise the gold film would simply fall off even at the lightest touch with equipment or with gases passed over during the experimental procedure.

Secondly an adhesion layer is necessary as if there is not one present the gold film and silicon interdiffuse rapidly create an alloy rather then the pure sample required [20]. If the gold is not pure then at the annealing stage the dewetting temperature and the temperature at which grain boundary formation starts will be inaccurate and not give consistent results. The prevention of the interdiffusing is required at room temperature. However some adhesion layer diffusion into each surface is necessary at the bonding temperature [4].

There are two different types of adhesion layers in common use. They are titanium and chromium. At present no differences are known in the different uses of chromium or titanium as an adhesion layer.

The adhesion layer does prohibit the gold and silicon diffusing into one another but the adhesion layer itself can as well, rather then diffusing into the bulk material the adhesion layer diffuses through the gold film at the grain boundaries

The diffusion of the adhesion layer through the gold film at the grain boundary occurs during the annealing stage. For the purposes of this project the adhesion layer to be used is chromium for the majority of the experimental work.

It does however have some dependencies, for example the diffusion through the grain boundary is dependent on the angle at which the grain is at. This has been proven for zinc as the adhesion layer diffusing through aluminium's grain boundaries [21].

The reason for stating earlier that a thinner film would be more beneficial then a thicker film due to evaporation of the gold and the adhesion layer because long term annealing of the film leads to complete depletion of the continuous chromium adhesion layer, therefore creating a near uniform through thickness gold-chromium solid solution. If this were the case then having accurate reproducible results would become a problem.

A thin film of titanium oxide on titanium can be used as the second adhesion layer. The gold and titanium interdiffuse rapidly and the titanium out-diffuses along grain boundaries and quickly oxidizes at the surface of the gold. Therefore stable titanium oxides can be formed on the surface of the gold [22].

So both adhesion layers show similar properties with respect to the diffusion of them through the gold layer.

Chemical Bonding Between Layers

The samples being created consist of four layers in an approximate basic model. These layers are the silicon wafer, SiO_2, chromium adhesion layer and the thin gold film. These are the layers that will be the basis of most experimental work and the bonding process that occurs between them is mixed oxide bonding [3].

Of the three series of samples that will be used throughout the investigation two are thought to have similar bonding patterns. The samples are gold with either the chromium or titanium adhesion layer. The third sample is of the gold film directly onto the silicon substrate. The bonding is now different as the two materials separately have high melting point for gold is 1064°C [31] and the corresponding temperature for silicon is 1414°C [23]. When the two materials have been evaporated directly onto one another then they

form a eutectic bond [24], [20]. It is when the two materials form an alloy together thereby lowering there effective melting point to ≈363°C. The eutectic bonding of the two materials will only occur when the two materials are evaporated directly onto one another. The lowering of the melting temperature to 363°C thereby gives the starting of the dewetting process at much lower temperatures, and so gives a control sample. The control sample may then be used to test and probe the prosperities of the difference in the adhesion layer. Figure 7 is the phase diagram for a gold silicon system is shown below.

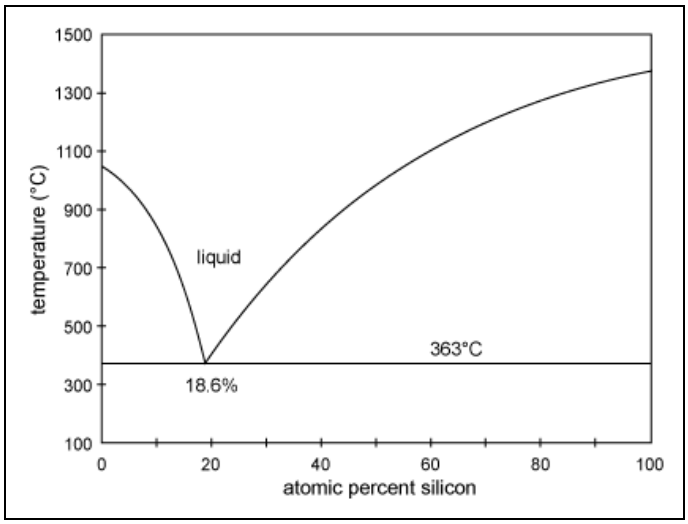

Figure 7: Phase diagram of the gold silicon system [25].

The phase diagram shows the mixing of the alloy of the silicon and the gold. The melting point of the alloy is indicated. The temperature is specific to a mix of the two elements at 18.6 atomic per cent of silicon, because gold is a very much heavier atom of the alloy in comparison to silicon [25].

Chapter 3

Experimental

For the duration of this project four different samples will be used to investigate every aspect of the crystal synthesis from the thin films.
The four samples all vary differently and are so for different purposes. The samples are as follows:

1) 20nm Gold + 2nm Chromium
2) 20nm Gold + 2nm Titanium
3) 20nm Gold (no adhesion layer)
4) Ramped sample 100-~0nm Gold (no adhesion layer)

The experimental procedure is comprised of three parts.

-Silicon wafer cleaning and evaporation of films.
-Annealing process of samples.
-Imaging and chemical analysis under Scanning Electron microscope.

The samples 1-3 are all created in the same way with only a different adhesion selected or the bypass of this layer evaporation altogether. Sample 4 is created in a different fashion. This sample was specifically brought in from United States of America.

For details on where experimentation took place see Appendix 1.

The following experimental methodology is for the production of samples 1-3, more specifically sample 1 as 90% of the data will be collected using this type of sample.

Wafer Cleaning (Piranha)

The purpose of cleaning the silicon wafer is to remove all dust particles and foreign bodies from the surface of the silicon wafer which can clearly be seen. The purpose of this is for a number of reasons. A clean evaporation of the adhesion layer and gold film onto the substrate at the intermediate layers and also on the sample surface. Particles that

are present on the sample may contribute to anomalous results as the dust particles are much larger then that of the randomly orientated gold crystal, therefore during and after the annealing stage the dust particles are most likely to cause ambiguities and irregularities leading to inaccurate results.

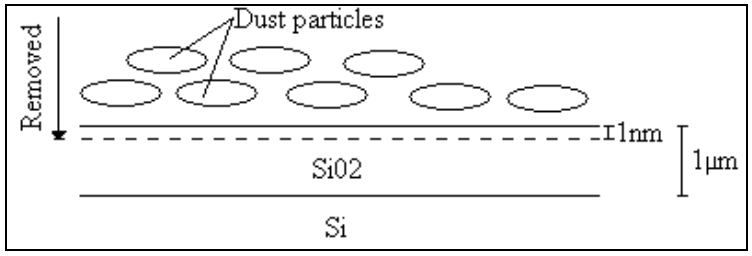

Figure 8: Showing depth as to which cleaning goes to remove dust particles on silicon wafer.

Figure 8 shows at the macro scale what the cleaning of the silicon wafer actually does. The cleaning of the wafer removes all dust particles that were present on the sample surface and also removes approximately 1nm of the silicon dioxide. The removal of the 1nm silicon dioxide will not be affected as this will grow back but gives a flat uniform base upon which the films can hence be evaporated onto providing a flat as possible film.

Method

It is essential that the wafer is kept as clean as possible. This also means the area that the sample is being prepared in.
The work area should be cleaned firstly using de-ionised water and a dust free cloth wipe so as to ensure no deposit of particles onto the work area, the cloth must be wetted with the de-ionised water as prevention against previous unknown experimental spills.

Remove the wafer from the storage box, in some cases it would have been stored in nitrogen to keep the wafer clean, and then place in a covered Petri-dish thereby making the sample easier to handle.
The handling of the sample must only be done with a pair of tweezers with a minimum area as possible on the wafer surface itself.

Using two beakers of minimum 800ml size the "piranha" solution can approximately be measured out. The quantities are 600ml of sulphuric acid (H_2SO_4) at 96% and 200ml of hydrogen peroxide (H_2O_2) at 25-30%. The quantities stated need only be an approximate measurement and there is no need for specialist equipment, it can be measured out by eye in the beaker as long as the ratio between the two chemicals is 3(H_2SO_4):1(H_2O_2).

Once the hydrogen peroxide has been added to the sulphuric acid the solution reaction will start to produce hydrogen and oxygen. The solution will start to "bubble" so should not be covered up. The reaction is also an exothermic reaction and highly oxidising, resulting in the solution giving off heat as the reaction progresses. The solution may reach quite high temperatures to the touch.

The silicon wafer can then be taken from the Petri-dish again using tweezers and placed into a wafer holder and fasten securely in place. The wafer holder enables the entire wafer to be cleaned without risk of dropping as the wafer is secured around the edges, much like you would handle a CD disc. The process cannot be achieved with tweezers as the area in which the wafer be supported would not be cleaned.

The secure wafer and holder then must be placed into the solution of sulphuric acid and hydrogen peroxide, the wafer needs to stay in the solution for approximately 10 minutes.

After 10 minutes the wafer and holder are then transferred to another beaker which has been full of de-ionised water, this is to allow the wafer and holder to be rinsed of all the H_2SO_4 and H_2O_2.
The rinsing of the wafer needs to be repeated a minimum 5 times with each time exchanging the beaker for clean de-ionised water, frequently this process may be repeated more.

Once the washings are completed and while the wafer is still in the holder it is advisable that the wafer is dried. Dry the wafer by use of the nitrogen gun in the laboratory. When drying the wafer the air gun must point towards the floor, reasoning being the nature of the cleanroom. The cleanroom has air ducts at the ceiling which blow down filtered air

which catches the dust particles and these are extracted by vents at the floor level. If the nitrogen gun were aimed upwards then it would be against the natural flow of the laboratory and a higher probability of dust particles landing on the wafer sample.
It can be observed when the wafer is dry as there is a slight colour change on the wafers surface.
When dry the wafer can be removed and placed back into the Petri-dish.

The process that was used for the cleaning of the silicon wafer can also be extended to the quartz boat sample. The only differences in the two methodologies being for the boat sample requiring a larger beaker with a wider base due to its shape, and also there is no requirement for a holder as no difficulty removing the boat sample from the solution.

Evaporation of Films

The next stage of the sample making procedure is to evaporate the metal films onto the wafer. This includes both the chromium adhesion layer and the thin gold film.
There are two methods in which the metal films can be deposited onto the silicon wafer, either splutter deposition or by evaporation process.
For the purposes of this project only the evaporation process will be investigated, this will be done through the use of an AUTO 306-Bell Jar Evaporator. This is also a low energy process. [26]

Method

The apparatus needs to be vented. This can be done via the touch screen display on the front of the apparatus. This vents the jar enabling it to be removed to allow for the wafer to be loaded.
The bell jar and the metal plate can be removed allowing the silicon wafer to be attached to its underside. The wafer can be held in place with tape. Once completed the metal plate can be reinserted back on the apparatus.
Whilst the bell jar is removed the gold crucible and chromium filaments can be checked ensuring that there is enough gold and chromium for the run of the apparatus, if not then this can be replenished.

Once the wafer is securely insitu then the bell jar can then be replaced back onto the apparatus ready for the evaporation process.

When replacing the sample holder and wafer there is a detector suspended further inside the apparatus, the purpose of which is to monitor the rate at which evaporation occurs, it requires a clear line of sight to the boat or crucible, without which the apparatus will cease to function.

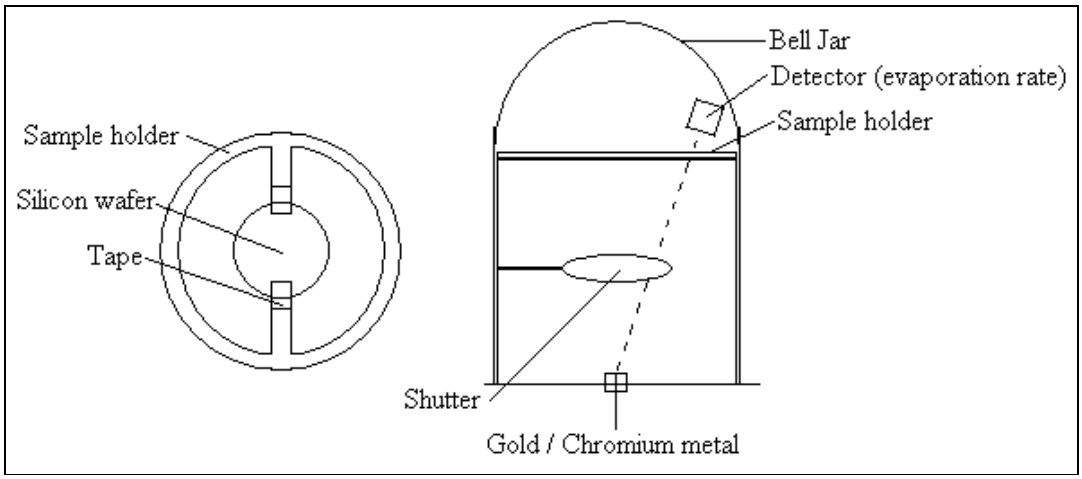

Figure 9: Diagram showing the bell jar and apparatus for the evaporation of the thin metal films.

Figure 9 shows the location of the silicon wafer inside the bell jar and the various components of apparatus that are essential to the evaporation procedure.

The vacuum pump can now be started so that the pressure is lowered firstly through roughening and then through fine (thermal) pumping ready for the evaporation process to start.

The disadvantage of this procedure as opposed to other type of evaporators is that the disc which the sample is attached to does not spin. The advantage of this feature is that it ensures that there is an even coating of the evaporated metal. The arrangement described here does not contain a rotating disk therefore there is a very small probability that there will be an uneven coating of the gold film, therefore allowing more of the gold deposited at the centre then at the edges as the boat containing the gold is directly below the centre of the sample, error measurements on the equipment show a possible 1nm change in thickness arising from this factor.

Once the bell jar has reached a low enough pressure, on average $1.5X10^{-7}$mbar, then the settings for evaporation can take place.
The voltage for the chromium filament during the first stage of the experiment for the deposition is set to 30V and set to a low tension.
Subsequently changing the current very slightly so the needle on the analogue display gives a slight "wiggle", the purpose of which is to ensure a good contact between the contacts and the rotating crucibles. The apparatus should be checked that the shutter is closed over the crucible or filament to prevent the evaporation of any metals before the procedure is ready.

The ammeter can be turned up to just below 4A for 1 minute to allow all impurities to be evaporated off and to ensure an even evaporation to establish. The ammeter is then increased further till a rate can then be measured, then press run on the automatic shutter. The automatic shutter can be programmed so that the shutter closes and evaporation terminated at the programmed 2nm for the first layer thereby obtaining accurate film thickness. The rate for the deposition of the chromium layer is $0.1nms^{-1}$.

For the evaporation of the gold layer the crucibles need to be rotated via a handle so that the gold boat is below the sample. The voltage being applied across the gold boat now needs to be changed to 10V then the same process is repeated. Check the connections via the ammeter but the current needs to be just below 3.5A. The current can then be increased till a rate is established then the gold is observed to be molten in the boat and the automatic shutter is activated and also altered so that it is activated when the thickness reaches 20nm.
The rate for the deposition of the gold layer is approximately $0.04nms^{-1}$.
Upon completion of the evaporation procedure the apparatus should be left at high vacuum for approximately 30mins to ensure metals have cooled. The evaporator can then be vented bringing the sample back to atmospheric pressure. The wafer is then cut into quarters and stored under nitrogen therefore ensuring as clean samples as possible before experimentation.

For the evaporation of the gold-titanium samples effectively the same method is used. The only difference is that the apparatus is changed to allow for the change of adhesion layer from chromium to titanium. The apparatus used for gold-titanium sample is the AUTO 500 E-beam evaporator.

Annealing of the Gold Film

The stage of annealing the gold films in the experiment is to develop the gold film into the randomly orientated crystals. This process firstly occurs at the grain boundary between the gold grains. To determine the temperature at which the grain boundary first appears various samples need to be annealed in the furnace at different temperatures and then analysed using a scanning electron microscope.

To place the samples into the furnace and ensure that they are removed correctly without damage they can be placed on a quartz boat. This therefore ensures the samples can be removed safely. Quartz is used and not glass because quartz can withstand temperatures of up to 1200˚C whereas glass at high temperatures is malleable due to its impureness and so would bend and flex leading to inhomogeneous annealing.

For the purposes of this project the annealing stage of the experiment, the time length of the sample in the furnace will remain at 1 hour and below 850˚C. This is because the samples already being observed above 850˚C. This investigation is much more interested at the low temperature annealing and also above this temperature the SiO_2 layer starts to grow and increase in thickness. The time length will remain fixed as rate of dewetting depends upon both temperature and time so to minimise the variables time will be held constant.

Method

The first action for the annealing process is to cut the silicon wafer into the correct size pieces thereby enabling them to be loaded into the furnace.

The silicon wafer can be cut through by using a diamond tipped pen and a pair of tweezers. Breaking the silicon wafer along the crystal grain edge with tweezers at one end and the pen across the opposite side of the wafer and then applying pressure. This

method of breaking the wafer ensures that the wafer can be broken with the minimal production of dust that can settle, and reduces damage to the gold film.
The alternative way of cutting up the sample is to use a dicing saw. This allows the samples to be cut into uniform shape and size, but the disadvantage is that is causes the gold film on the surface of the wafer to crack so therefore cannot be used.

Once cut to the correct size the samples can then be cleaned by having the residual dust blown off the sample by use of the nitrogen guns.
The next step is the preparation of the furnace ready for sample loading, the glass tube needs to be replaced so that there is no cross contamination from other oxides in the furnace (other experiments).
To proceed disconnect all the connections from the ends of the tube; it is at this stage that the open ends need to be covered thereby reducing the contamination of the tube. The previous tube can now be removed and the process then reversed for reassembling of the furnace. The “gold” tube put in place with the ceramic “O” rings placed at either end of the gold tube approximately 1cm within the furnace’s edge. These ceramic rings are in place to prevent convection currents within the furnace. Remove each end of the tube covers so the tube may be connected to allow gas flow through the tube. The tube must now be approximately central within the furnace.

The fittings are now be attached to the tube. These will connect to the gas flow apparatus and consists of firstly a brass ring slid onto the tube 1cm from the end again then two rubber rings placed adjacent to the brass ring. A stainless steel locking ring is then attached, this secures the gas flow apparatus to the tube. These connections need to be made to both ends of the gold tube. It is at this point that the sample must be loaded into the tube.
The correct size samples are placed onto the sample boat, this ensures that while the samples are within the furnace they have a flat base whilst annealing takes place, convection currents around the sample and non-flat samples can cause ambiguities in the silicon wafer. The revealed ambiguities are apparent as stress and strain marks on the wafer and a non-uniform dewetting of the gold film.

Once the samples are on the boat they can be loaded into the centre of the gold tube within the furnace, this is accomplished by using a glass rod pushing the sample on the boat to approximately the centre of the furnace. The last of the gas flow apparatus is then assembled, another rubber ring with attachment to the gas flow is placed next to the locking ring with then a clamp enclosing the last few apparatus pieces securely in place and ensuring an airtight vacuum.

Figure 10 shows the gold tube and the fittings made to connect the gas flow to the apparatus. The connections that can be seen in figure 10 need to be made to each end of the gold tube. The furnace for this project uses nitrogen as the inert gas which flows through the gold tube although other gases such as Argon, Oxygen may also be used.

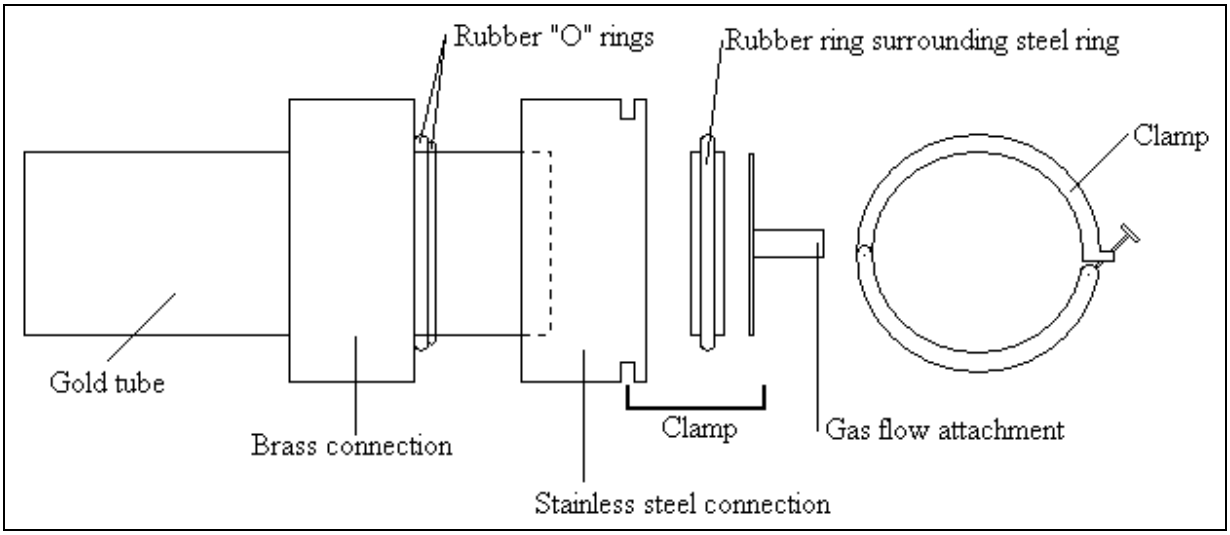

Figure 10: This diagram shows the apparatus set up for furnace connections.

The gas flow rate and quantity need to be programmed so that 100% of nitrogen flows at 500sccm. The temperature control is programmed so that the correct temperature is reached for the right amount of time. The furnace is programmed to allow it to sit at room temperature with no heating for the first 30 minutes to ensure purging of the system with the nitrogen (See Appendix 2).

The rate at which the temperature is increased must be programmed at a rate of 5°C per minute until the furnace reaches the desired temperature which is then programmed. The

furnace will run for 1hour, after the time has elapsed turn off and allow the furnace to cool naturally to the ambient room temperature.

Once the samples have cooled within the furnace they can then be removed by the same process by which they were loaded with the glass rod. Once removed the samples can then be placed using tweezers into a plastic case ready for using the scanning electron microscope to analyse the stage of dewetting the gold film is at.

Scanning Electron Microscope (SEM)

The imaging of the gold films after the dewetting stage of the sample is to allow observation and to determine what stage the dewetting of the gold films is at, and therefore to analyse if the furnace temperature was set at the right level for the grain boundary formation.
Chemical analysis of the samples may also take effect at this stage from X-rays emitted from reflected electrons from the sample by elastic scattering and so by spectrum comparison.

Method

The first stage of the preparation for the loading into the SEM is to secure the sample using black carbon tape to the mount which can then be placed into the metal plate, the black carbon tape is effectively double sided sticky tape. Once applied to the plate the sample can be pressed gently onto it using a pair of tweezers. The samples and the plates to which the samples are attached can then be attached to the SEM control disk. This enables the samples once inside the SEM to be rotated or tilted as necessary. Figure 11 shows how the sample is mounted ready for the SEM to take place.

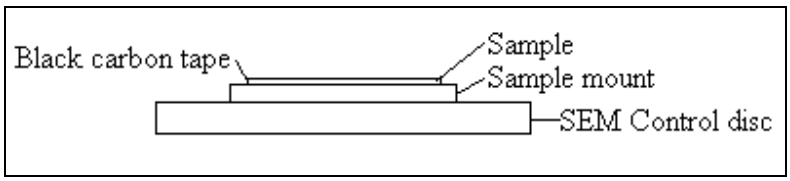

Figure 11: Mounting the sample

The SEM control disc is screwed onto a rod attached in the airlock. Once the airlock door is shut and locked in place the chamber can be pumped so the pressure is equalised. Once the pressure is equalised the airlock can be opened and the sample pushed into the main chamber where the rod attaching the control disc is removed to enable movement within the chamber. To ensure the control disk is secure in the chamber and correct in position there is a live TV feed so the placing of the sample is correct.

At this stage the pump on the vacuum chamber may be witched off, this enables better resolution as the vibrations will no longer disturb the sample.

The sample must then be placed so that it is under the electron beam using known coordinates and the electron beam switched on (open column chamber valve and switch on EHT gun). The view is then changed to SEM1 or INLens, this will then give a black screen. To view the sample the settings may need to be changed for example the brightness, contrast and also the focus and magnification. If however this does not work then the sample may need to be brought closer to the tip of the SEM, it is best to view the live feed again so as not to collide the sample with the e-beam tip. The electron beam can have set working distances, so the beam is in focus a distance x mm from the gun. This means placing the sample at this distance will give a high focus of the beam. Directly after the sample is found the settings can then be used to adjust the image seen on the screen. There are other settings which now become more relevant. They include for example the speed rate at which the surface is scanned, and the stigmator. The scanning rate is important as it is proportional to the resolution of the collected image, the slower the scanning rate the better the final image. The time taken for each scan will be much longer and there is the possibility of the sample moving inside the vacuum chamber which can be viewed on the image. The stigmator is for fine adjustments for the focus of the image.

The area of which the SEM's focusing can be reduced, this has the advantage that the smaller area to focus and magnify is a much quicker process for the adjustments, then once the settings are at an optimum they can then be applied to a larger sample area.

The final image can now be saved.

This process can be repeated throughout the sample, using the X-Y coordinate's to move the sample as required. The sample may also be rotated by an angle θ with respect to the horizontal plane. Once completed the reverse needs to be applied, so the control disc is

removed via the rod back into the airlock. Then the procedure changes, the option to vent the chamber is now chosen as well as opening the valve to the nitrogen gas supply. This will allow the flow of nitrogen into the airlock thereby bringing the pressure to normal atmospheric pressures allowing the sample to be removed.
The method above is that described for London Centre for Nanotechnology SEM. A field emission SEM from the Institute for Archaeology will also be used for which the method varies.

The main differences between the two SEM's is that the SEM at the Institute of Archaeology has a sample mount with a lip so is not necessary for samples to be stuck down, secondly has a lower resolution.

Chapter 4

Results

The results are listed in each experimental run in regards to the temperature the samples were annealed to. This is done as it presents a chronological path on logical thought processes from previous results.

Experimental Run 1

Samples Used

Three samples were used for the first run of the experiment. Two of which were created in the cleanroom and one other was imported from United States of America. The two samples which were created in the cleanroom both have chromium used as the adhesion layer and which measures approximately 2nm. Then both samples have a gold film evaporated onto the chromium, measuring 20±1nm using a profilometer to measure the depth of the gold layer. The two samples were then cut to $1cm^2$ ready for furnace loading. The third sample used for the first run was imported from United States of America, the sample was dissimilar from the other two and less is known about it. The third sample is a ramped sample of varying thickness, with no adhesion layer present on the sample.

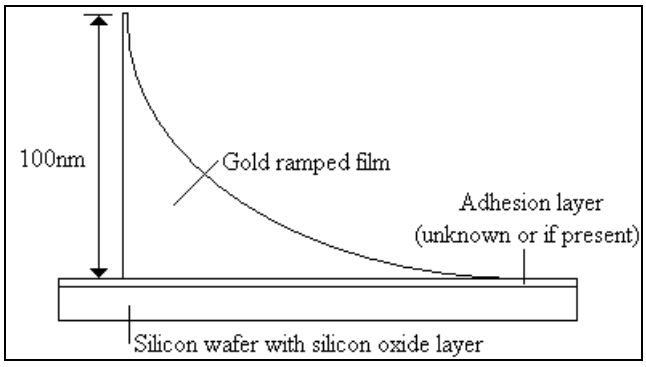

Figure 12: Diagram showing the ramped gold film sample.

Figure 12 shows the third sample used in the first run of the experiment, this sample has a ramped thickness which has an exponential shape. This thickness varies from approximately 100nm to zero. The advantage of using a sample which has varying

thickness is that the sample may cover a range of temperatures. The sample will show the different stages of dewetting due to the change in thickness. It should be observed that as the SEM moves towards the thicker end of the sample the grains should become less dewetted whereas at the thinner end should be further along to crystal synthesis.

Positioning of Samples

The positioning of the sample within the furnace is also recorded so that once the SEM has been taken of the samples the images collected can be related to their position within the furnace and if any abnormalities are observed using the SEM. The positioning of the samples may prove important in order to relate to any convection currents or unknown phenomenon.

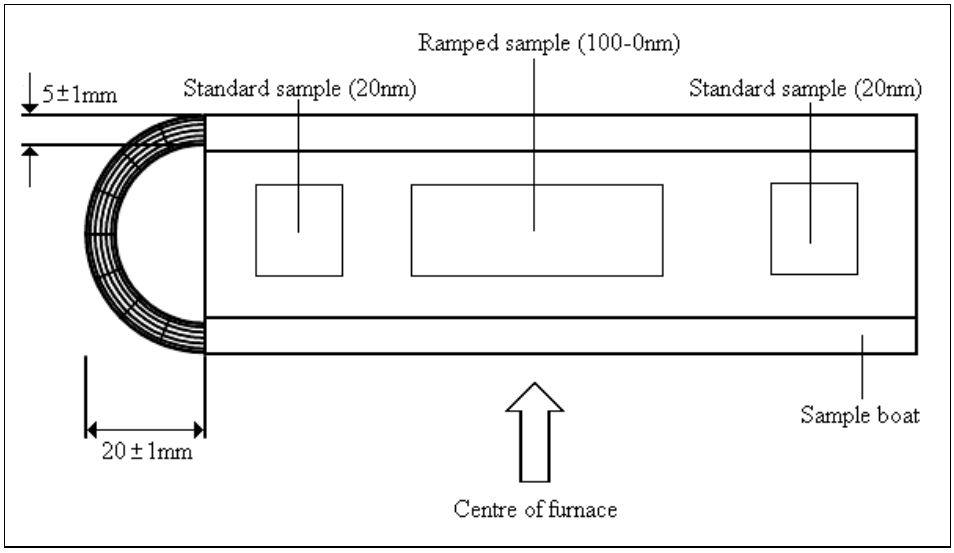

Figure 13: Sample boat to be placed within furnace and position of samples.

Figure 13 shows the sample boat loaded and the position of the samples.

The first run of the experiment set the temperature of the furnace to be ramped at 5° per minute with the constant temperature set to 650°C for one hour then after which the furnace will automatically turn off allowing the furnace to cool to ambient room temperature.

Placing more then one sample per run in the furnace is because there are two varieties of samples within the furnace so this would enable a comparison can be made between the

samples and the effect the materials used has on the dewetting rate will become more apparent. The second reason for placing two samples from the same batch is in effect a repeat of the same temperature. This is done in the same furnace run as the apparatus is heavily booked by many personal thereby limiting available experimental times.
Within the furnace there is a high temperature gradient with respect to position of the sample in the furnace during the annealing process. However a change in position along the sample boat (short range) should not be subject to a change in temperature due to gradient of the furnace.

SEM Images

The three samples were then analyzed under an SEM and images taken. Each sample had a number of images taken and the position of that particular image on the sample recorded so that a comparison can be made if necessary.

Ramped Sample

The diagram below shows the relative positioning of the SEM images taken on the ramped sample. The numbers that are, for example: 1-4 show that the images taken were in the same location but with the magnification, contrast and the focus changed.

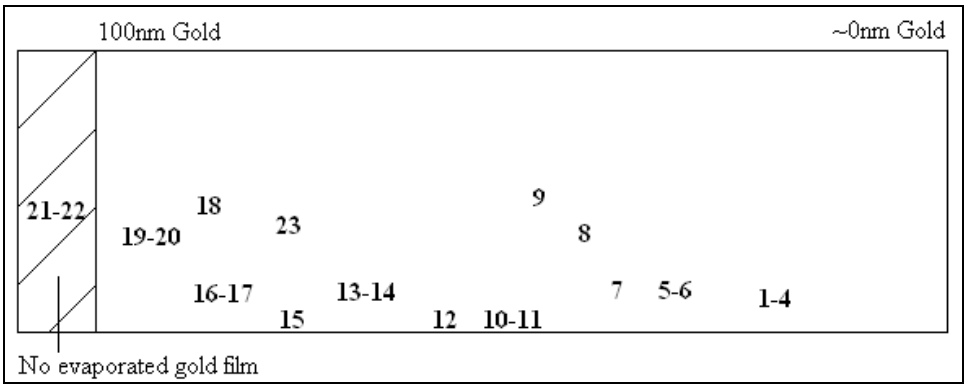

Figure 14: Diagram showing the relative positioning of the SEM images taken for 650ºC sample. (Refer to appendix for complete set of images).

Figure 15 shows an SEM of the ramped sample that was placed in the furnace at temperature of 650°C for duration of one hour.

It can be seen in the image that the sample has been successful annealed so that the thin gold film has become almost fully dewetted. There is a large majority of single grains randomly present, with only a few regions where the grains are still together such that rivers are present but to a size of only a few crystal grains in length.

It is noted that as the randomly orientated crystals are not immediately next to one another the crystals have changed shape and have moved away from the nearest grains. It is at this point that if the annealing is continued then the grains not only do they move further apart from each other but the height of the crystal grains also increases as the process continues. It is at this stage that coarsening and coalescence take effect to diminish the smaller grains found throughout the sample. The image quality prohibits the grain boundary to be visible. This is an issue as grain boundary structures are difficult to distinguish from in between grains. Randomly orientated gold crystals are present but they are order of size ranging to approximately 100nm. These are the size much larger the thickness of the film which is ~20nm. The crystals were originally flat plates and when in this phase had grains of approximate a size similar to that of the thickness of the film. The grains then coalescence and coarsen together to form the larger crystals which is seen in the image. The shape also gives further rise to the evidence of the random orientated crystal grains that are seen.

There are other structures present larger then ~100nm in size but are of such a shape that it can be assumed they consist of more then one grain present. The reason being is that the structure has river like properties or the anomaly has a smaller grain/randomly orientated crystal pulling away so a figure of eight shape is clear along with the grain boundary associated with it. These grain boundaries are visible when others are not due to the size of the grain boundary being relatively large. To be able to see the smaller grain boundaries on the SEM image the magnification and resolution has to be increased dramatically.

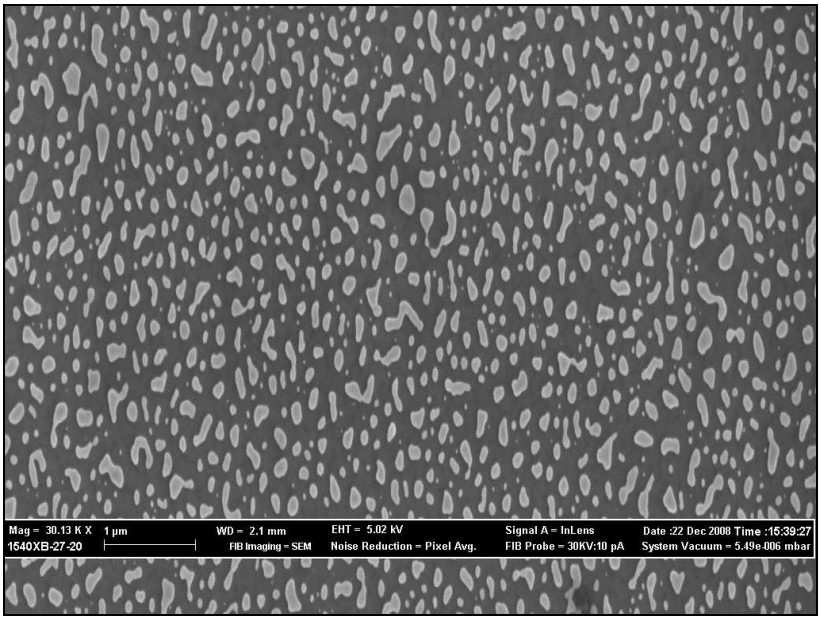

Figure 15: Image showing SEM of ramped sample. (Position 2)

There can also be further analysis on the image other then qualitative. Using the ImageJ and GIMP programmes (See Appendix ImageJ, which are both image software packages), can then extract the information within the greyscale image which the SEM produces.

The greyscale image is one which each pixel has an X-Y coordinate and an associated relative intensity.

Through the use of both programmes the structures can accurately be measured and the area of each gold particle analysed.

Graph 1 shows how the programme was used to obtain a distribution of the grain size for the 650°C Ramped sample. This distribution clearly shows an average grain size for the 650°C sample to be approximately 50nm in size. This shows the grains coarsen and coalescence before and after the formation of the grain boundaries and the break up the gold grains.

The error associated with the measurement of each grain is comprised of two parts. Firstly the error on measurement of the grain recorded and secondly the error on each pixel. This is because each pixel has a set distance X dependent on the magnification of

the microscope and so over this distance no detail of when the grain stops can be collected

The orientation that the grains were when measured in is of particular importance. When the longest orientation of each grain is measured for the distribution, it yielded a distribution which has a lot of noise and not a clearly defined shape or peak of average grain size (Appendix 4). In comparison graph 1 has a clean positively skewed distribution. The orientation of the grain size for the length recorded was horizontal to the image collected from the SEM.

The reason the distribution is much clearer when the grain measurement is taken horizontally is due to the sample plane's normal not aligning with that of the sample mount's normal, thereby meaning the resultant image is skewed in either the X or Y coordinate. Further evidence to this is when the same sample is imaged again under a different SEM there appears to be no stretching of the sample (due to non-aligned sample) when the two images are compared (See Appendix 5).

The sample's plane not being parallel to that of the sample mount is most likely due to the black carbon tape placed underneath to secure the sample, whereas the second SEM comprises of a sample boat so no tape is required leading to a higher accuracy of smaller scale structures and not at risk of image skew, but there is a loss as there is no conductive tape underneath so the sample is more likely to charge making the image collection more complex.

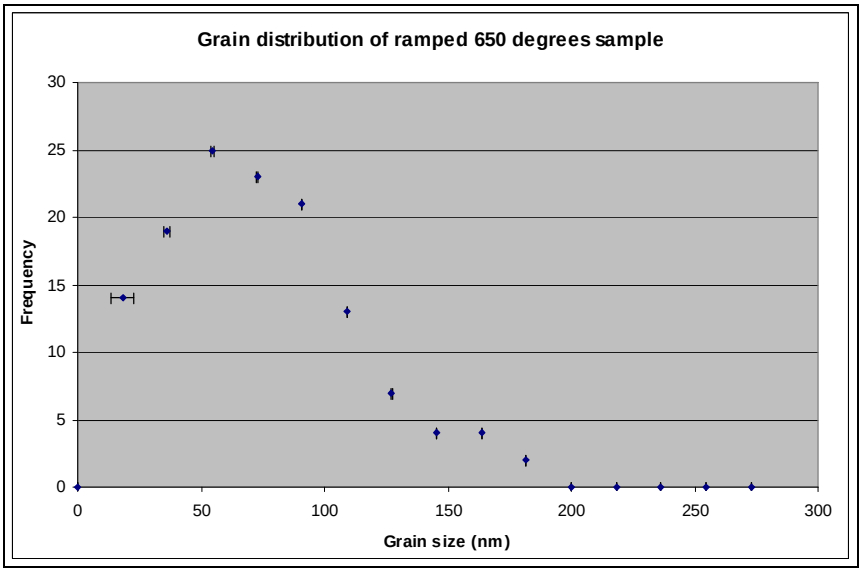

Graph 1: Graph showing the grain size distribution on the ramped 650°C.

Using figure 15 the percentage of gold coverage of the image can be calculated, this was found to be 25%. It is calculated under the assumption that no gold coalescence or coarsened from outside the image view as this was taken for the original film area and that the grain height is binary so grains are seen as a cylinder not sphere for a first approximation.

Taking into account that the metal films and the substrate base all have associated thermal expansion coefficients for the image size calculated for the percentage gold covered thermal expansion increases the percentage coverage of gold to 26%.

The relative intensity in the greyscale image collected can also be used to give a diagrammatic representation as to the surface morphology of the film.

Graph 2 shows the surface profile of gold grain using the relative intensity in one dimension.

Next to the grain profile figure 16 shows a three dimensional image of the same gold grain. It has been created using both spatial coordinates (X and Y) and using the relative intensity as the third to plot the image. It is easer to see how this model overestimates the percentage of gold coverage as the gold grain is in reality spherical or prolate spheroid in shape. The detail about the grain base has been lost as the image has been taken parallel

to the normal of the substrate surface. It means the 3D image is assumed to be only correct to the mid-way point on the gold grain in the Z direction.

A more accurate way of analysing the profile of the gold grain would be to use an Atomic Force Microscope. This gives a topographical image of the sample surface by use of Van der Waals forces between the microscope tip and sample.

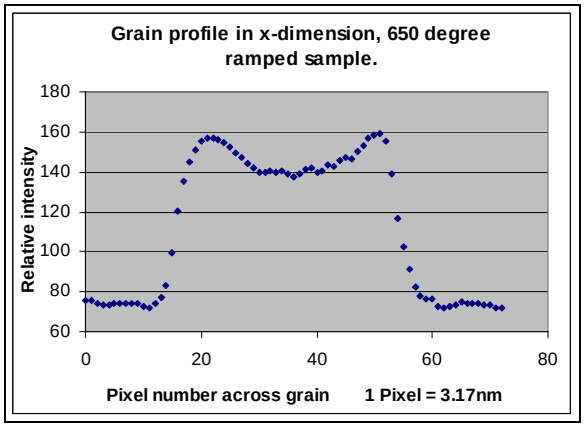

Graph 2: Graph showing the Grain profile.

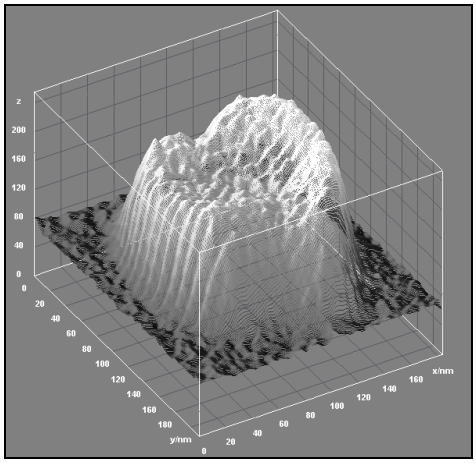

Figure 16: 3D image of top half of gold grain.

Figure 17 is another image from the same sample. The main difference from this image to the previous one shown is that the position has been changed to three quarters of the way along the sample. Therefore this means that the gold film is now thicker. The consequence that this has on the dewetting of the film is that there should be fewer crystals and more of the rivers and plates. To achieve break up of the large plates similar to figure 15 either the temperature needs to be increased or time which the sample which is exposed to the temperature, as the dewetting rate is dependent on both.

The image clearly shows large areas of apparent flat gold film with no visible grain boundaries this is most likely due to the magnification being insufficient. There are areas of smaller plates which appear to have broken away and become subsequently smaller. There are areas where smaller plates seem to be sitting are in an apparent hole. There seems to be no reason why this has occurred as it would normally be found at the edge, the film surrounding seems to be seamless so no boundary migration from the main film break-up.

The image was taken at position 15 on figure 14, thereby the image is along one edge of the silicon wafer. The edge of the sample in figure 17 is on the right lateral image side. It can be concluded that as the gold film approaches the edge of the wafer the thickness of the film seems to increase. Thereby causing the large plate when in comparison to moving towards the centre of the film is the film has progressed further towards dewetting and an apparent even thickness of film as the general size of the rivers and grains is consistent.

Figure 17 also shows to be what looks like bright large grains spread throughout the entire image. These are not singular grains as their size can be anything up to 2μm therefore these must be groups of grains which are sitting above the plane of the gold film, so are much larger in structure. The reason for these structures to appear brighter then the rest of the image is from electron scattering from the SEM beam.

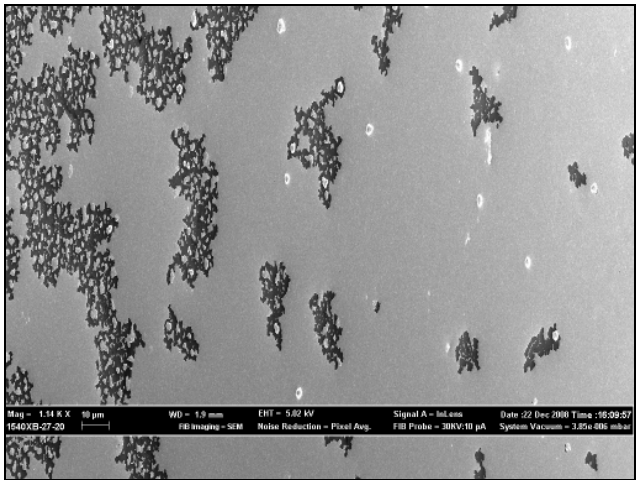

Figure 17: Image showing SEM of ramped sample. (Position 15)

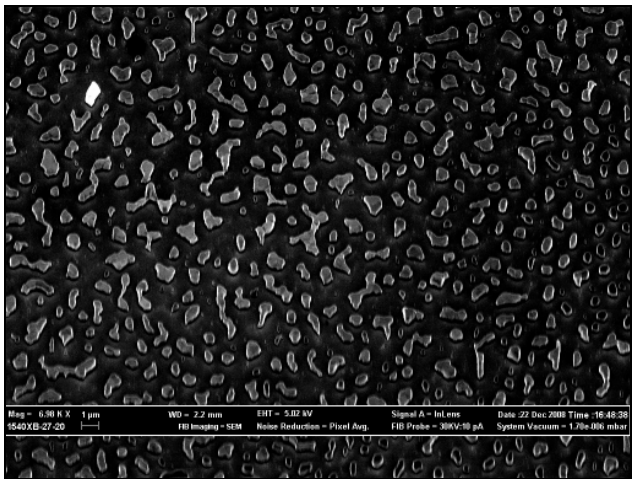

Figure 18: Image showing SEM of ramped sample. (Position 21)

The final image shown here of the ramped sample, figure 18 is again of the thin gold film nearing the fully dewetted stage of the annealing process. The fundamental difference between this image and figure 17/15 is the location at which it was taken. This image was recorded at location 21 which was thought to have no gold film whatsoever as it was past the thickest part of the film and no gold is visible (A thin gold film is visible to the naked eye even when at thicknesses of 20nm. Though not as a gold colour as the penetration

depth is such that some intensity of visible wavelength light is reflected, so the silicon wafer can also be seen through the gold film giving the mix of colours). The conclusion that can be made from this is that there is not a sudden end to the gold film but a ramp down as well. This ramp must have a relatively high gradient as the size of the crystals decreases rapidly over a short distance.

There can be seen smaller crystals in the image as well as collective grains of rivers. Grain boundaries can also be seen as the image is of a better quality and resolution.

The size of the randomly orientated crystals is misleading in figure 18 due to the angle which the image was recorded. The sample was tilted at an angle of 45° to the horizontal plane to the previous images. The advantage of tilting the sample is that it gives the image some depth and makes for observing the grain boundaries easier as they are no longer perpendicular to the observer and so the groove is visible.

The figure also depicts again a bright structure so therefore has scattered the electrons more then the surrounding crystals.

The overall analysis of this particular sample including all the images is that the sample has either been annealed for too long or the temperature is too high. It was surmised that under the correct conditions just large flat plates to be seen, but higher magnifications show some grain boundaries are visible. This sample has had the grain boundary completely broken on the large plates with only fully formed randomly orientated crystals present. The sample also does not contain any form of adhesion layer. Therefore a decrease in the rate of the dewetting of the gold to crystals will be observed for samples with the adhesion layer as its purpose is to bind the gold to the silicon wafer more efficiently.

The preparation of ramped samples is elaborate and the film thickness cannot be controlled accurately. Therefore to investigate the formation of gold crystals from thin films more systematically, substrates were coated with a constant thickness of 20 nm gold film (which is known to form single 200 nm nanocrystals of Au (111) when annealed at 1050ºC for more than 10 hours)

Standard Sample (20nm)

The two standard samples were placed in identical places equal distances from the centre so the same effects should be seen.

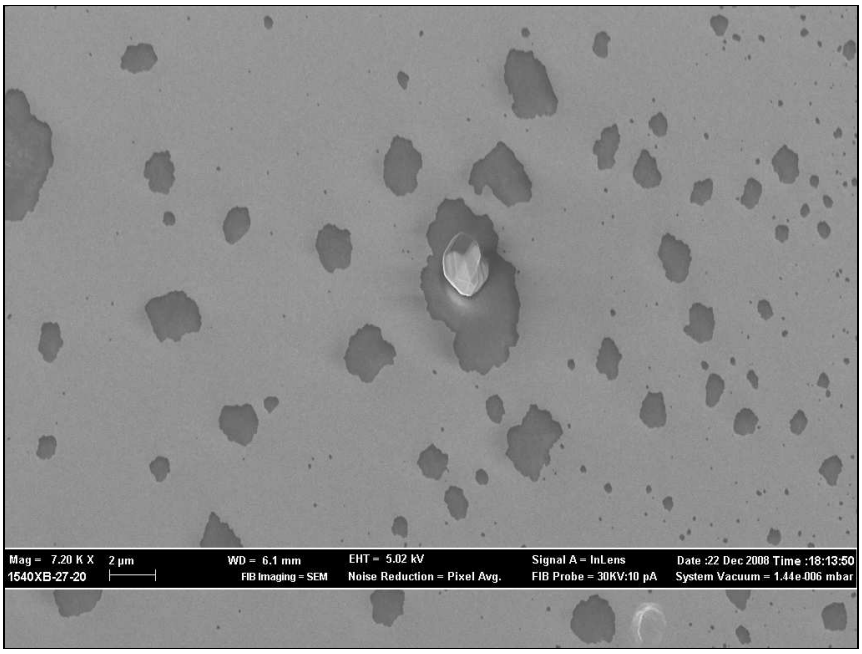

Figure 19: Image of the first standard sample (20nm), pitted Gold layer with single gold crystal.

Figure 19 is of one of the 20nm samples created. It shows the sample surface being pitted with a large number of holes through the gold layer through to the oxide layer underneath.

This is unexplained as the holes were thought to be associated with abnormalities with the silicon oxide layer which would not occur at this frequency. The hole abnormality is observed in both of the samples present.

It was seen that as the SEM moved towards the edge of the sample in both cases the number of holes increased as well as the average size of the hole increasing

Observation of the image is primarily the gold layer, but with a series of holes present varying in size to over 2µm in size.

The only crystal that is visible is located in the centre of the image on figure 19. The crystal that is seen can be described as a large crystal that has reached the end of the

dewetting process. This can be said as the crystal has fully formed facets on the top and its size is that approximate to 2μm in length and 1μm in width and so is much larger then the expected 200nm in size for the average random orientated crystal.
It can be expected that for an original film thickness of 20nm then the average crystal size will be 200nm, so the size of the crystals is on average 10 times larger then the thickness of the film.
It appears to have a series of lines going across the crystal. These are most likely due to line defects within the crystal. The most likely defect that can be seen by that of the SEM is the edge dislocations on the side of the crystal. These are due to the termination of a plane of atoms in the middle of the crystal, therefore the other arrays of the atom planes in the crystal bend round this defect thereby giving what can be seen in the image. There is one more unusual quality of figure 19 which is apparent in the majority of the SEM images for this sample. It is visible that for most of the crystals that have remained all reside in the holes of the chromium adhesion layer, to my current knowledge this has not been observed and so there can be no definitive answer to the reasoning behind it.

Figure 20 shows effectively the same trend as figure 19. There are a large number of holes in the gold layer with large gold crystals present, most in holes.
The holes vary largely in size. The inset image in figure 20 shows one of the crystals at a much higher magnification then the previous images, thereby giving a clearer image.
The position of the fully formed crystals has been highlighted via the square, the positioning is important as for both the standard sample's both only had the crystals forming near the edges of the silicon wafer and not to be located in the sample centre. The distribution of the gold crystals across the sample surface can start to be seen over the distances that the image shows.

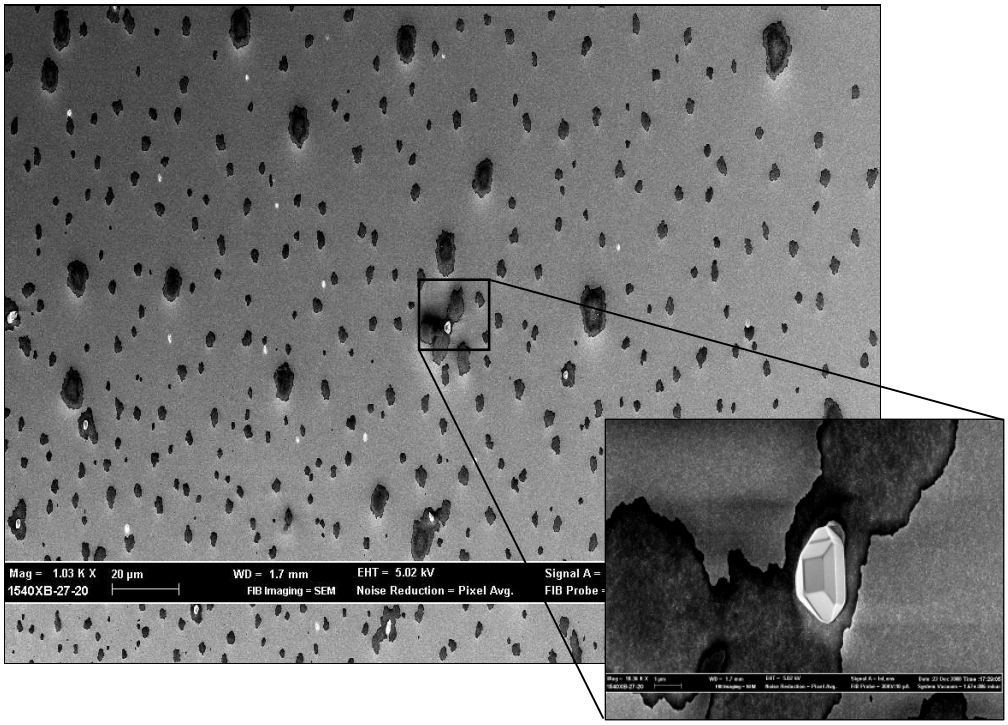

Figure 20: Image of the first standard sample (20nm). Inset: Gold crystal fully formed, position marked with square on lower magnification image.

The similarities between this crystal and from figure 19 are very pronounced as again the crystal is approximately 5 times the size of the expected 200nm size, and the facets and defects are visible. The grain boundaries on both samples are not visible, but the holes that are forming on the sample surface are present and so seem to be a process of the annealing process.

The images show no evidence of any gold break up so the percentage of the hole coverage is more relevant. The holes cover 6.9% of the sample under observation for figure 20.

Experimental Run 2

The first experimental run effectively determined the temperature of the furnace as being too low, or not running for long enough time for the observation of the grain boundary formation. However if the hole formation in the samples is part of the grain boundary formation then the temperature of formation will be lower. Therefore the temperature for this run will be lowered to 300°C. It then creates a temperature range for a more exact reading at which the grain boundaries/hole formation first starts and so provide a limit on the range available on the gold film breakup.

The procedure of build up to the temperature will be a repeat of the previous set of samples, so the temperature will be ramped to increase at 5°C per minute and then to hold at the designated temperate for a period of on hour. The cooling down of the samples will however be different as during the intermittent time between the experimental runs information yielded that when the temperature reaches the higher temperatures such that of the first experimental run (650°C). Once the furnace is switched off the temperature will drop a few hundred degrees in the first few minutes. This is not the most accurate method as this rapid drop in temperature cannot be controlled and any effects that it may have on the grain boundary or gold crystal formation is unknown. To counter these affects once the furnace has completed the required temperature for the hour then the furnace will ramp the temperature down again to 200°C less then the constant programmed temperature at the same rate until it reaches the new temperature value. Once this is reached the furnace will turn off as before and allow cooling naturally, the temperature will then be low enough so that the change in temperature with the ambient conditions is small enough to ensure no rapid cooling of the samples occurs.

Samples Used

The second experimental run required a new set of samples to be cut from the silicon wafer created. This is one more variable that cannot be controlled within the confines of this project. The variable arises because the silicon wafer can only be cut once the

evaporation has taken place and then can only be cut using a diamond edged pen not a dicing saw.

This introduces the possibility of dewetting process dependent on the sample size as no two samples will be in the approximate same size range. The effect would be more predominant in the larger sample size as the conduction to the sample centre would take a greater time in comparison to a smaller size so therefore the centre of the larger sample should not have progressed as far into dewetting.

The second run used three samples as of a similar set up to that of the first. It includes two standard samples of size ~1cm^2 placed at either end of the sample boat, with the third ramped sample placed in the centre.

The ramped sample again is of unknown exact thickness and with no adhesion layer.

The positioning of the samples is the same as that of figure 13.

SEM Images

The three samples are then imaged individually under the SEM to observe their structure and the stage at which they have annealed to.

During the SEM analysis, in search for the most relevant images to record the results for further analysis the on-screen images brightness slowly decreased until no longer visible. The phenomenon occurred at each new location the SEM was scanning regardless of the settings the operator applied, yet once the position of the sample was moved the dark region moved with the sample thereby giving once again a clear image. This provided the evidence that was the sample surface being burnt during the scanning process by the electron gun. Further evidence for this is the magnification at which the SEM is set, because the rate at which the burning occurs on the sample increases with magnification applied to the sample surface. This presents the problem that the potential grain boundaries present from the temperature the samples were annealed at are very small and so require a large magnification to be seen. In order for these structures to be seen successfully if present, particular areas of the sample were destroyed through burning of the surface to allow for focusing. The SEM would then be magnified as required and focused until the on-screen image is black, the sample moved along to a clear area of sample then the process is repeated. This is done until the required image is collected.

Why the SEM appears to burn the sample surface is unknown, as the electron gun is set at the same voltage as the previous experiment (known as data recorded on each image). The difference between the first and second run SEM settings was those that would only decrease the beam intensity with distance. These are such as distance from the sample to probe and the pressure within the chamber. A possible solution to this problem would be that upon focusing the SEM to the smaller structures is that there is an electron beam induced deposition. This is the deposition of carbonaceous material over the sample and "welding" of them to the sample. This can lead to small surface structures being buried in seconds and at low accelerator voltages becomes extremely obvious [29].
It was also seen on the live image that as time progressed the image tended to move across the screen, this is due to the sample becoming charged as both the thin films and the silicon substrate are highly conductive and for the images collected the samples were not earthed correctly.

Figure 21 shows an image of the ramped sample placed centrally within the furnace. The black squares that are observable in the image centre are where the SEM apparently burnt the sample surface scanning during a magnification. In comparison to the last experimental run where most of the gold is fully dewetted the image here shows the gold film to a large degree still intact with no areas of breaking up or of the rivers forming.

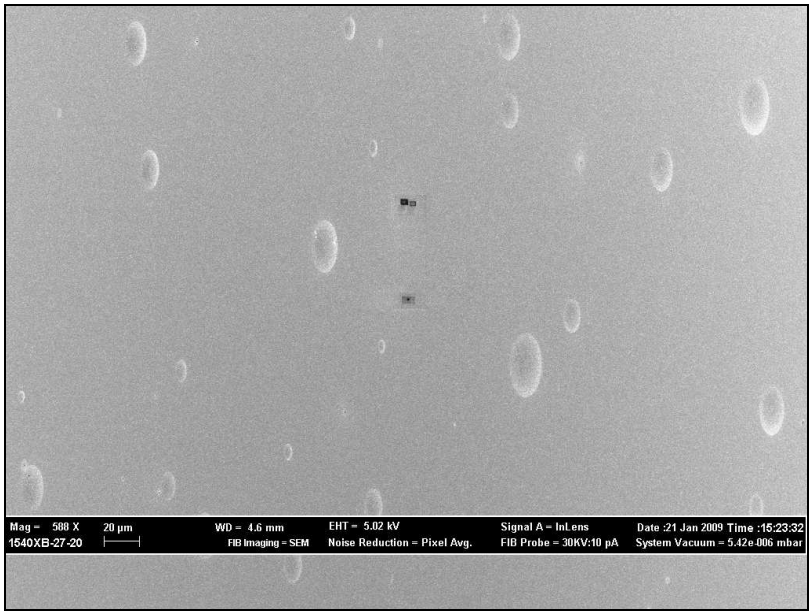

Figure 21: Image of ramped sample (300℃).

The sample also shows a series of oval structures scattered throughout figure 21, they are of a size ranging from the nanometre scale to over 2µm in size and appear to be raised above the surface of the plane of the gold film as shown in the image which has had the contrast altered to emphasize this affect. These anomalies are only partially scattered throughout the sample and are mainly confined to the thicker parts of the gold film. The sequential images taken along the length of the sample showed a decrease in their number until the random areas of gold dewetting started then none of these structures were visible at the size scale that was seen at the thickest end of the sample gold film. It can be seen they have a drop like structure and therefore can be said it is a contaminant of some kind before the evaporation of the metals onto the substrate occurred.

The sequential images mainly showed the gold film without any evidence of dewetting having occurred. Only when the SEM tip has reached approximately two thirds of the sample length does any form of the dewetting process become visible. This is of the form of local isolated regions where the plates have started to separate to form cracks, these will then develop further to form rivers and eventually randomly orientated crystals. However as the thickness of the film at this location can not be said with any great accuracy then this temperature cannot be said as to when the film starts to dewet.

The two other standard samples placed in the same furnace run were analysed under the SEM and showed no thin film development at all. There were no grain boundaries present or holes. The only structure visible was occasional holes due to holes in the oxide layer. These were distributed throughout the sample as first approximated and appeared every few mm. the shape of these structures also confirm the holes being due to the oxide layer.

Experimental Run 3

The previous results of the annealing of the samples at 300°C had put an effective range on the observable temperatures for further experimental runs. The individual grains are visible but are of order size expected to be after the evaporation process with no annealing process taking place (20nm). There are no grain boundaries visible.

Samples Used

The following set of samples will then be taken to a temperature of 500°C under the same conditions of the previous runs and the same settings. It will then minimise any introduction of new variables. The samples to be used are two from the same wafer that was created.

SEM Images

Figure 22 shows the image of the 500°C sample after the annealing process. The image's contrast and brightness have been altered so that the structures are more prominent. It shows the same hole like structure that is apparent on the 650°C sample. The holes that are present are not as often spread throughout the sample as previously, or are the size of the holes as large as the higher temperature samples.

It is observed that as the number of holes have decreased with a reduction in the applied temperature then a relationship between both number of holes and the average area is clear. It can then be assumed that if this occurs at other temperatures then the formation of the holes is a property of the annealing process of gold film on chromium.

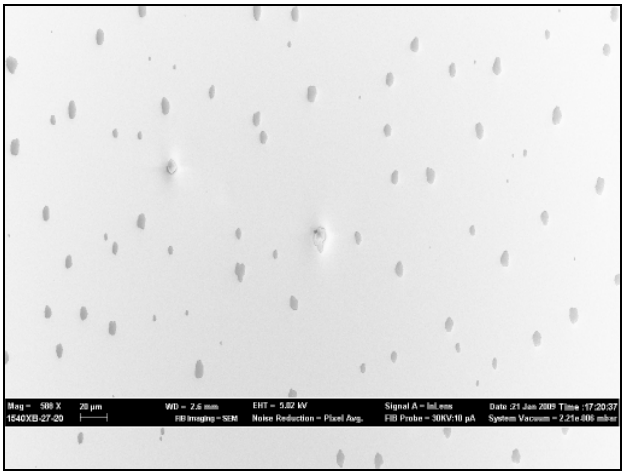

Figure 22: Image of standard sample (500℃) Brightness and contrast altered.

The holes visible in figure 22 were viewed in both of the samples placed in the same furnace during the same heat treatment process, which again suggests that it is a property of the annealing process.
The percentage of hole coverage at 500°C is 1.9%

On further inspection of the holes at much higher magnification it can be observed that the shape is not of a uniform shape and seems to be on average circular but not as clearly defined as the holes associated with irregularities in the oxide layer. On higher magnification the holes viewed, show that there is some structure to the holes themselves.

Figure 23 shows the higher magnification image of the edge of a hole. For the majority of the image the gold island can be viewed and at closer inspection the individual gold grains seen. In the bottom right corner of figure 23 shows inside the hole and the same grain pattern in the hole can be observed as that on the gold island. The fundamental difference between the two being that no gold is present within the hole. When the size of the grains in the hole and in the gold islands are measured then compared the grains in the hole are 105% of the size of the gold grains, and so appear larger than the gold grains at the same temperature.

Without any compositional analysis or further evidence of this structure at different temperatures there can be no definitive answer as to the nature of this phenomenon, and its relevance to the dewetting of the thin films.

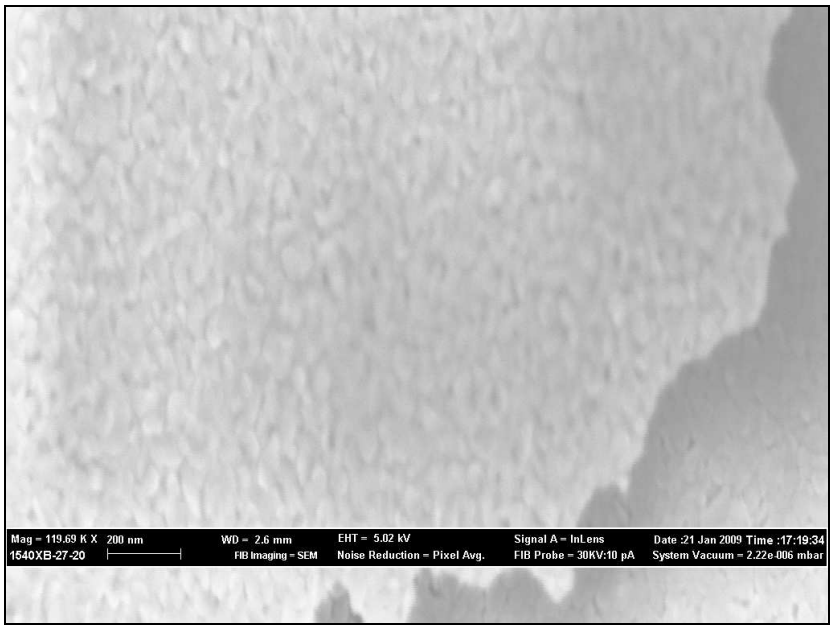

Figure 23: Image showing the edge of gold island with hole and grain boundary structure on both areas of the sample.

From the 500°C sample although the individual grains are visible the groove formation is yet to be observed, as is the coarsening and coalescence process of the grains to a larger size. The grains as viewed in the above two figures still show consistent grain size with that of the 300°C sample which is of order ≈20nm in size.

To provide further evidence for the hole formation being a property of the annealing process a standard sample with no heat treatment having taken place was imaged under the SEM. The result is that as expected no holes or any irregularity was observed on the sample (See Appendix 7).

Experimental Run 4

The 650, 300 and 500°C samples all having been viewed under the SEM have all so far shown no grain boundary behaviour but increase in hole number with temperature.
The temperature applied to the samples for this experimental run was increased to 750°C so as to achieve an upper limit on the range in which the gold film starts showing grain boundary formation and the dewetting process leads to a break up of the gold film.

Samples Used

The samples used for this experiment are from the same wafer and will be annealed under the same conditions. The temperature the samples will reach is 750°C. As the temperature is much higher then previous, the sample will need to be ramped in both directions, thereby prohibiting thermal shock.

SEM Images

On removal from the furnace inspection of the samples under visible light shows some shadowing of the sample around the edge where there appears to be no gold. It is either that the gold has evaporated from the sample leaving the bare substrate, or that the gold has progressed further into dewetting at the edges thereby forming the small individual grains or crystals, which cannot be seen using visible light.

Figure 24 shows the SEM images collected from the 750°C sample. It is shown clearly that the gold film is no longer the flat plate as it was at 650°C, therefore this gives a range of the temperature that the samples can observe for the formation of grain boundaries to occur.

Observation reveals that the gold has started the dewetting process and the grains are coarsening and coalescence together thereby majority of the gold film has formed isolated islands. As well as the island being more prominent the gold grains are of much larger size in comparison to lower temperatures. The grain size is on average 90 nm in X direction.

Previous temperatures of 650, 500°C showed hole formation increase with temperature, the 750°C sample also maintains that trend. The holes are not directly observable when no longer bound by the surrounding gold plate, however they can be observed when the relative positions of the isolated crystals, grains, and plates are taken into account.

The percentage coverage of the holes on the sample is 59.4%

This is a large change in the area of the hole coverage. Therefore an operator error associated with that value. The sample no longer has defined edges for the holes the programmes used required a clear boundary. Achieving that boundary the image threshold for the relative intensity needed to be changed to the optimum viewed image, thereby giving clear edges to the holes. The disadvantage of this technique is its dependence on the brightness and contrast recorded for the image collection leading to loss or gain in data that was not previously present (See Appendix ImageJ).

Figure 24 highlighted where there were previous holes before the dewetting process continued which now leaving the bare substrate void of gold structures. The substrate which is more observable as the gold has coarsened and coalescence into individual islands shows the same structure as with the 500°C sample, there is a grain boundary formation over the entire substrate. It again shows the grains to be of order size ≈20-50 nm these cannot be measured to any greater accuracy as firstly the structures are too small and secondly there is no consistent shape or defined edges (See Appendix 8).

Figure 24 shows a zoom on a crystal in the image. The crystal is seen to be fully formed as its size is to the micron scale. It is a fully formed crystal, firstly the surrounding area of the crystal shows no gold islands whatsoever, that is due to the grain growth processes that absorbs and eliminates smaller grains nearby. Second the crystal has fully formed facets, it is a process of crystallography and so as the heat treatment continues more of the grains will show this behaviour.

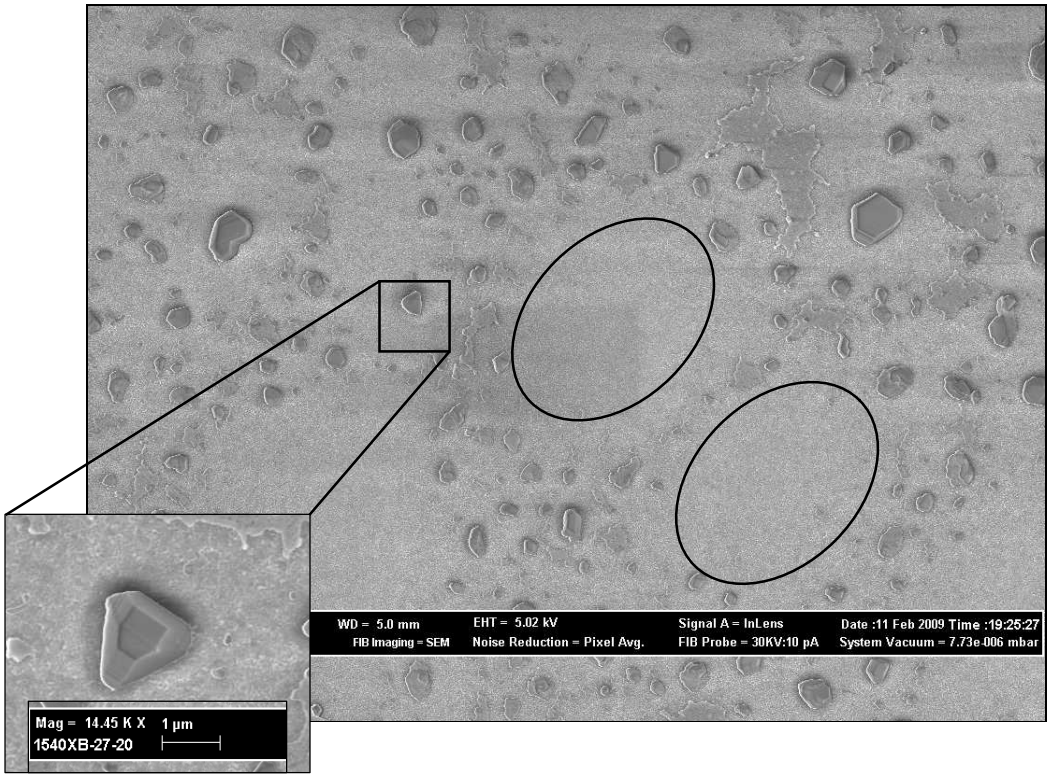

Figure 24: Image showing 750℃ sample; Apparent hole location defined by gold island shown by ovals. Insert: Magnification of single grain with facets forming.

The grain structure in the holes has been observed at 500, 650 and 750°C, a compositional image was taken of the 750°C sample. The benefit of this is that to allow specific areas of the live image to be analysed for the elements present in this region. The process is achieved through the use of Back-scattered electrons (BSE). BSE are beam electrons that are reflected from the sample by elastic scattering. BSE are often used in analytical SEM along with the spectrum made from the characteristic X-rays. Because the intensity of the BSE signal is strongly related to the atomic number (Z) of the specimen, BSE images can provide information about the distribution of different elements in the sample from the spectrum collected [30]. The spectrum being the photon count at each particular energy of the X-ray observed.

The BSE process works by increasing the beam's energy to above the energy required to excite the necessary element that is desired to be seen. Thereby allowing excitations of the atom to emit X-rays.

The process may then identify the elements seen in the images so as to confirm which film layer is under analysis.
In order to excite both the chromium and the gold metals both need a beam energy of 10-12 KeV, but 15KeV will be used to allowing for broadening of the energy levels and so to be certain of the elements being detected.
The image shown with the spectrum in figure 25 is of a poorer quality for imaging purposes as the energy of the electron beam was too high. It can cause problems with rapid charging of the sample's surface. This is when electrons accumulate on the sample surface thereby repelling further electrons aimed at the sample before any interaction occurs. For clear surface images shown for experimental runs 1, 2 and 3 lower beam energies of 5KeV was sufficient. The image is of poor quality due to it being a compositional image. It means that areas in the image appearing with a greater brightness are of an increased density and so therefore increase in gold mass present having progressed away from the grains to the crystal formation.

The spectrum in figure 25 shows the elements present during analysis of X-rays reflected from the surface. On inspection all the materials that are present in the sample can be seen. The reason that all the elements can be observed when the area analysed is less then the area of island is due to the energy of the electron beam. The beam is of energy 15KeV which when directed at the sample reveals an area surrounding the beam which will also become excited. In effect there will be a sphere of excitation at the point of contact of the beam with the sample surface of the surrounding atoms, even when the beam is focused to a point.

It is why silicon and oxygen can be observed when the gold plates are under analysis.
The characteristic X-rays that are emitted from the excitation of the elements have some degree of error as there are other elements within the periodic table that share this spectrum. The error is reduced greatly on the spectrum obtained as all materials present on the sample are known and are of high purity.

In figure 25 all the elements are labelled accordingly to the element present. The chromium peak is labelled differently according to its K spectral line. It is also a much

reduced peak in comparison to the others as the relative abundance of chromium is much smaller then the gold, silicon or oxygen.

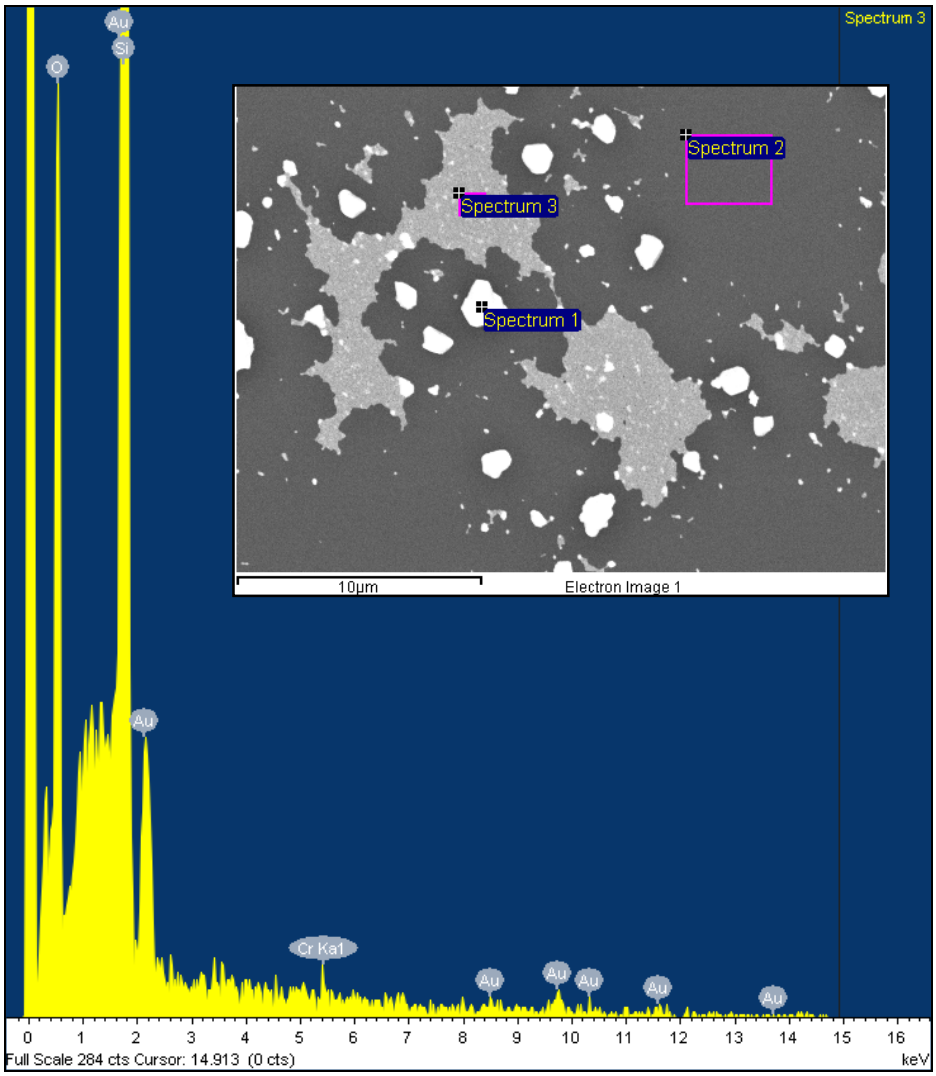

Figure 25: Spectrum showing element analysis of gold film in island formation.

Previous experiments using chromium as the adhesion layer indicates it may diffuse between the grain boundaries to the surface upon contact with air forms Cr_2O_3.

It then provides evidence to this process as the chromium peak is visible on the selected area where the film is intact, the chromium that is becoming excited is present on the surface leading to a segregation process having occurred.

The second area under analysis on the compositional image is that of spectrum two on figure 25. The spectrum for this region on the sample is shown in figure 26.
It is for the determination of the nature of the grain effect being observed in the holes at various temperatures.
The spectrum shows that there are large quantities of silicon and oxygen, which would correspond to the silicon oxide amorphous layer. There is also a peak of carbon present. The most likely explanation for this would be the reaction between the ambient air and the oxide layer.
The label for where the chromium peak should appear is marked on the spectrum at 5.5KeV. The peak for this particular value does not have a definitive shape above that of the noise spectrum therefore this cannot confirm that chromium is present.
Without the presence of chromium the structure observed on the substrate surface is purely from the silicon oxide layer.

The final spectrum analysed is that of a gold crystal (spectrum 1), this spectrum shows again the peaks for silicon, oxygen and carbon due to surrounding excitations. The peaks are correspondingly smaller than the gold peaks. There are two main peaks for the gold at 9.7KeV and 2.1Kev these are L and M spectral lines respectively (See Appendix 9).
The presence of the peaks confirms the increase in density of gold for the particular grain. It does not give any peak to the chromium adhesion layer, suggesting no presence within the gold crystal itself.

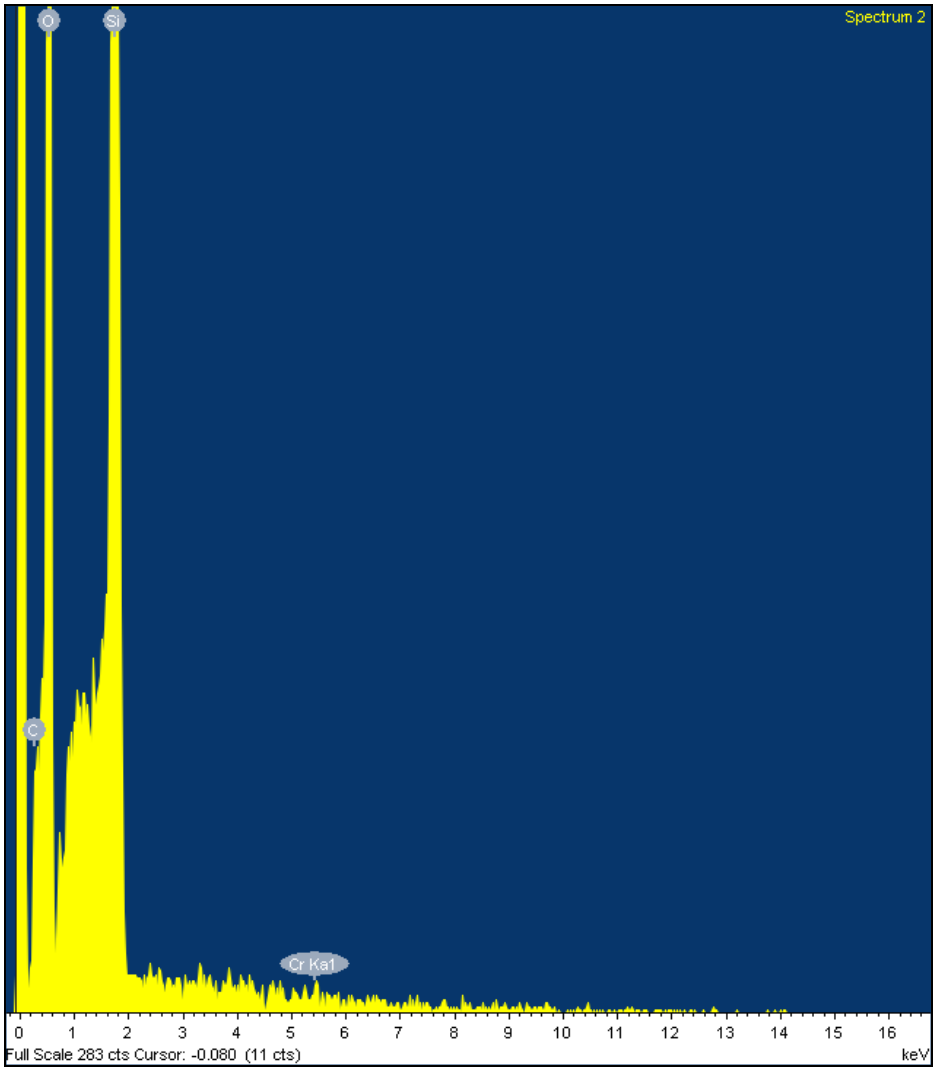

Figure 26: Spectrum showing element analysis of grain pattern on substrate surface.

The average grain size for the heat treatment of 750°C is 192nm. The grain pattern seen is thought to arise from chromium as the structure in the hole is 93% of the size of the gold grain within the same image. This evidence suggests that the structure observed is not associated with the gold. It would be expected that the grain anomaly would coalescence and coarsen at the same rate as the gold islands therefore giving the same average size. It is evidence that the grain effect seen on the holes on the substrate is due to the adhesion layer, this would mean that the chromium grains are leaving an impression in the silicon oxide as to there grain structure. The X-ray analysis is evidence that no chromium elements were present. The percentage of the grain boundary effect

seen in the holes in relation to the average gold grain size yields information that this is an impression in the silicon oxide. For samples annealed to a temperature of 650°C the grain effect in the holes is on average 121% of the gold grain size, it would suggest that the grain structure is decreasing with increase in temperature when in reality it would be the silicon oxide growth therefore reducing the contrast in the structure.

The overall result of the 750°C sample is that the temperature is too high for the grain boundary formation to be observed but has successfully found an upper limit.

Experimental Run 5

The samples and methodology must be kept constant while the temperature is to be held constant for an hour at 725°C then ramped down to 650°C.
The collected SEM images from the sample were again of a similar context to that of the images from the 750°C sample. It showed that the gold had advanced into the dewetting phase too far. Unlike the images from the 750°C samples the gold islands that remain in plate format are of non-uniform shape. The images suggest that a contaminant or a different operation occurred during the annealing process causing anomalous grain growth formation.

The images can still be used for the determination of the percentage of the hole coverage which was 20.2% but the samples will not be used for any further analysis.

A further sample that was present in the furnace. It was a sample that had shaped regions of gold on the surface formed by e-beam lithography. The shapes present on the sample were arrays of rectangular, triangular and rhombus dots each with varying areas.
It was carried out as an investigation into the process that shaped gold films go into and to observe if patterned samples show a similar process to that of thin continuous films [27].

SEM Images

The SEM images for the 725°C sample are shown in Appendix 10.

The SEM images of the patterned sample are shown in Appendix 11.

Experimental Run 6

Samples Used

The previous run determined the temperature being excessive for grain boundary formation. Therefore should be lowered to 675°C for the held temperature. The samples used for the experimental run would be of three different types. As the temperature of the grain boundary formation has been narrowed to a range of 650-725°C for samples with the chromium adhesion layer. The three sample used are:- Standard sample with 20nm gold 2nm chromium adhesion layer, 20nm gold 2nm titanium adhesion layer and the third sample is where the gold has been evaporated directly on the substrate.

Three different samples were used so that a comparison could be made between them, thereby giving an indication as to the effect the adhesion layers have on the progress of dewetting at a set temperature. The second reason is that the grain boundary formation for the gold-chromium samples occurs in the range 650-725°C so that the other samples may be analysed if they show similar properties at that temperature.

SEM Images

Following removal from the furnace the samples showed once more a shadow region around the edge of the sample as seen for 750°C samples. The conclusion that can be made from this is that this process is occurring from the samples observing an increase in temperature from the thermal convection of the sample boat. It would be due to the sample boat not being on a flat surface therefore the samples edges were in contact with the sample boat rather then the bulk.

Figure 27 shows the gold on chromium adhesion layer sample annealed to 675°C. The holes as expected were still present on the sample. However with the majority of the holes a crystal has started to grow at the centre or edge. If the sample was allowed to continue annealing at the temperature increased then more of the film would start to break up into individual grains and hence crystals.

The holes that are present cover an area of 25% of the image, again this shows the trend of increase in area coverage with temperature.

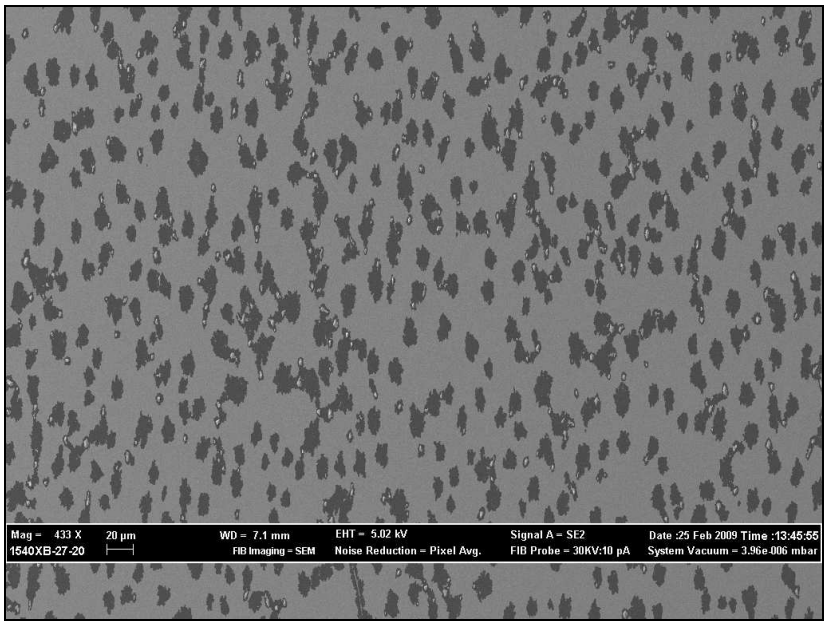

Figure 27: Image showing gold on chromium sample at 675℃

What also can be observed on the image and across the sample is that the starting formation of the crystals is relatively constant as the average number of crystals per hole is 1.43 and of the holes in the image approximately 35% are at this average value.

A higher magnification image of one of the holes edge can be seen in Appendix 12. It shows a similar trend to previous higher magnification images, it being the grain boundary effect on the substrate and also no clear grain boundaries visible on the film. The grain boundaries will be specifically hard to observe as the SEM works by observing the different contrast's observed through the relative intensities obtained. Therefore the grain boundaries are very small and can be of size 10's of nm or less then the contrast difference between the two adjacent grains will be very small and so difficult to observe the boundary.

In comparison with the gold on chromium sample would be a sample with no adhesion layer at all. It is informative as it shows a control as to the effect of no intermediate layer. The effect of no chromium layer is seen in figure 28.

Figure 28 shows the gold film at the mid dewetting stage, it is seen as there are no longer large island plate formations visible, only river and single grain/crystals are visible. The magnification in figure 28 shows the typical river structure, it is comprised of a linear array of grains whose interface energies keep them together. The grain boundaries are also clearly visible as grooves which transverse the full width of the river. Although the boundaries are visible the temperature is to be considered too high as randomly orientated crystals have already started forming. In comparison to the samples with the chromium layer which show an increase in crystal formation, therefore confirming that intermediate chromium acts as a adhesion layer through increasing the interface energies. The gold on the substrate samples also shows no hole properties. The missing holes would then suggest the formation of them to be a property of the chromium layer.

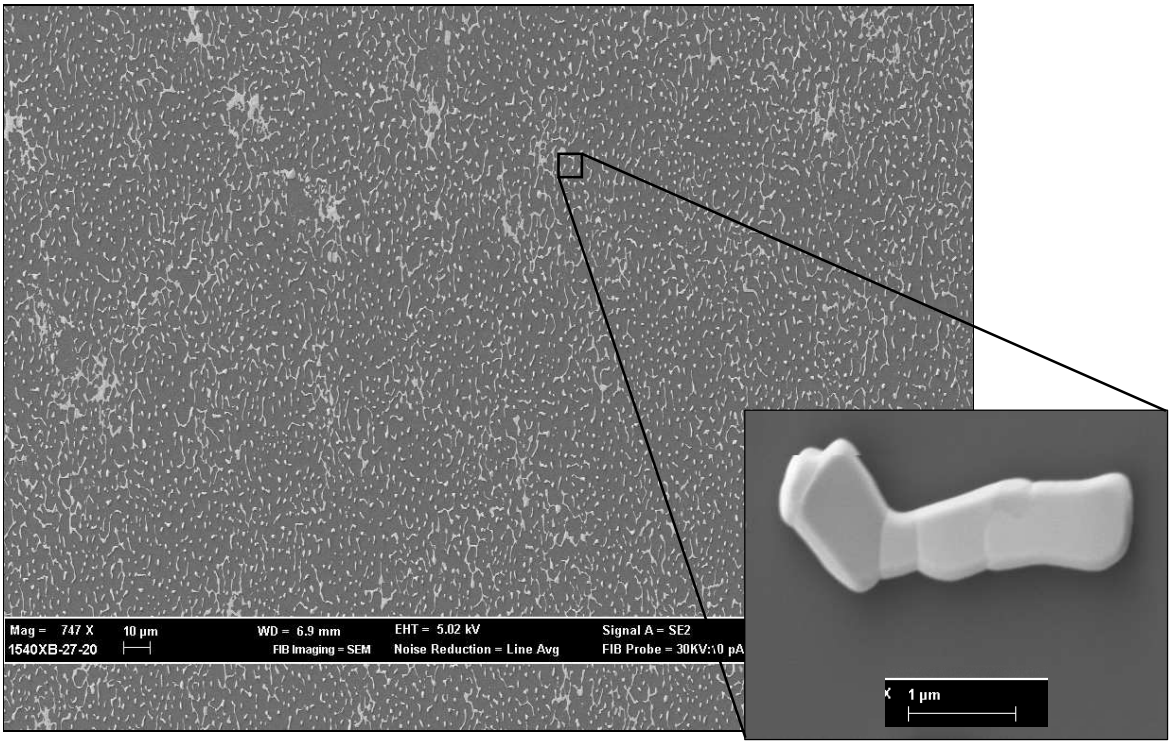

Figure 28: Image showing the progress of dewetting with the gold on silicon sample.
Insert: Gold river.

The second structure that cannot be seen is the grain pattern on the substrate surface. It provides further evidence to it arising because of the intermediate wetting layer.
The final of the three samples used for this experimental run is the sample with titanium replacing chromium as the intermediate layer.

Figure 29 shows the sample with titanium as the adhesion layer.

The first observation is that all of the gold is now in crystal formation and no grains are conjoined. The impact is that as all three samples were in the same furnace run with the thicknesses of the relative layers being the same the differences are due to the intermediate layer. The influence the inclusion of the titanium layer had is that it increases the rate of the dewetting of the gold film. The titanium can then be known as a surfactant layer. The implication is that the titanium layer will aid the dewetting in comparison to the gold on substrate sample which contradicts previous thoughts that this layer behaves the same as the chromium and so would increase the dewetting temperature to above that seen for the gold/substrate sample.

Figure 29 on higher magnification imaging shows the gold crystals far more advanced then any previous experimental data, as those crystals all showed multiple clear facets.

The sample at this temperature does not show any formation of holes throughout the sample but however does show the same grain like pattern on the substrate surface. It again is further evidence to the structure being caused from the adhesion layer.

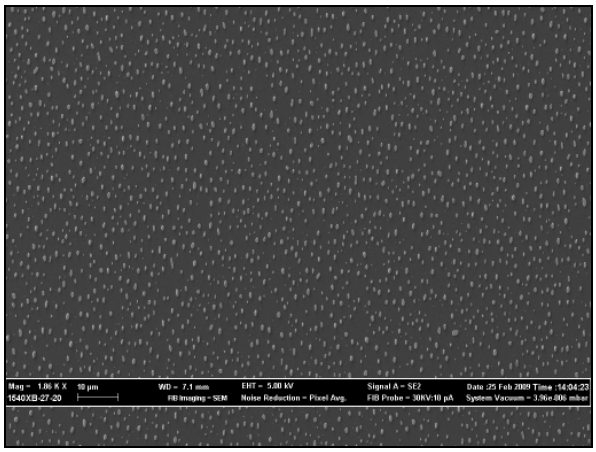

Figure 29: Image showing uniform randomly oriented crystals, on gold/titanium sample.

Experimental Run 7

The results were repeated when the temperature was lowered to 650°C for three more samples taken from the same wafer as the previous experimental run.

Samples Used

The temperature was set at 650°C, firstly to confirm the results seen in previous runs and secondly to compare the three samples again at lower temperatures. The three samples being the gold-chromium, gold-titanium and the gold on the substrate sample.

SEM Images

The differences seen between temperatures 675 and 650°C were very small. For the gold on chromium sample the difference was that there is no starting crystal formation on the hole edge, so the holes were more spherical in shape and again fewer in number. The percentage coverage of the hole for the repeat of the 650°C sample is 10.2% whereas in comparison with before the value was 6.9% which agrees with the earlier experimental run. The gold on substrate sample shows only a slight increase in river length, so a decrease in number of isolated grains.

The gold-titanium sample showed no change with respect to the change in temperature. The facets were still completely formed and the percentage of gold coverage for the 650°C sample is 15.6%. This does not agree with the higher 675°C sample at a gold coverage of 6.9% therefore showing a decrease in grain/crystal area and a gain in the height to an average value of 215nm.

It shows that there is no significant difference in the decrease of 25˚C of the sample whereas for both other samples an observation can be made as to the relative changes of the samples.

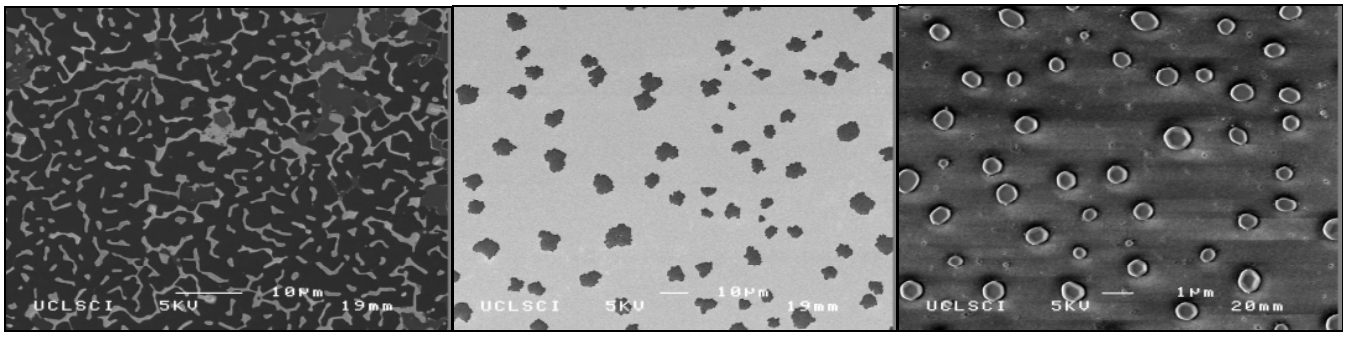

Figure 30: Three samples used for repeat of 650℃.
Left (Gold on silicon substrate); Central (Gold with chromium adhesion layer); Right (Gold with titanium adhesion layer).

The three images shown above in figure 30 are of the three different samples. They are the gold-chromium, gold-titanium and the gold on substrate samples.
The relative difference in the rate of the dewetting process can be observed.

The samples with the chromium adhesion layer showed with the secondary electrons that the chromium only appears to be present on the island formation. It was repeated with the titanium samples to see if a similar process occurs. Previously areas of the samples were analysed using this technique, however it can only be used as a qualitative result as the counts of the photons of X-ray radiation are only specific to each area of sample and so therefore are of no correlation to one another. For the analysis of the titanium sample a linescan across one of the single isolated island yields information on the distribution of the elements distribution across the sample.
A linescan is in effect the same as taking areas of the sample and analysing for elements, the difference being for the linescan is that multiple X-ray scans are recorded along the same line selected (See Figure 31) whereas an area analysis only observes once. Therefore linescan gives better resolution of elements.

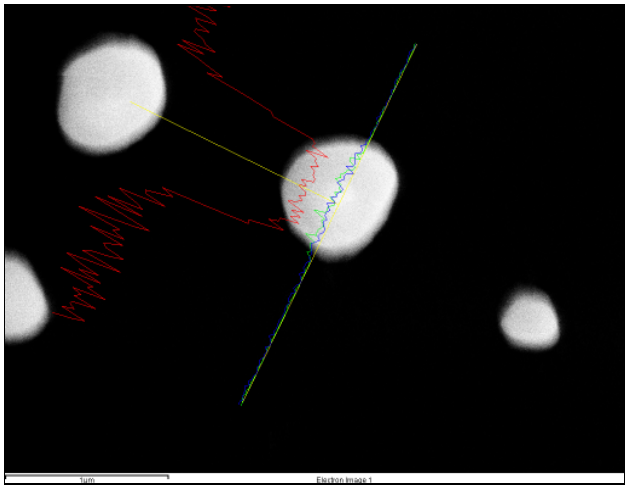

Figure 31: Image showing the linescan of the elements across grain of gold (sample having titanium adhesion layer).

Figure 31 above shows the three elements observed along the linescan which is the line at 45° to the horizontal. The three lines are that of the gold (green), titanium (blue) and of the silicon oxide (red). The silicon and titanium are that of the K line series whereas the gold is of L.

The figure below is of the same linescan, with a direct comparison between each distribution.

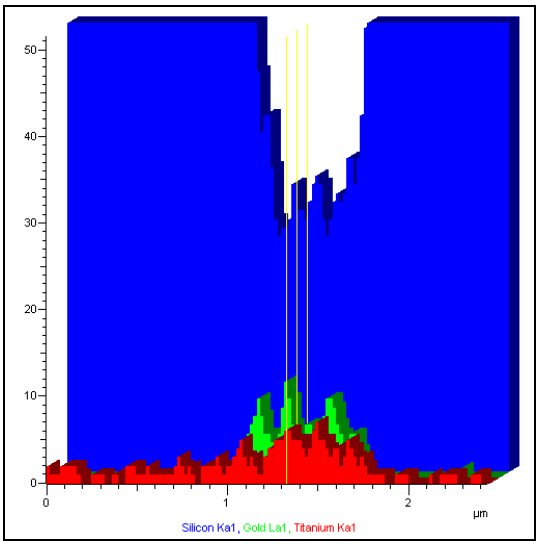

Figure 32: Distribution of elements across the gold grain.

The Blue distribution for figure 32 is that of silicon. It shows a decrease of this element where the gold grain is present as expected. In comparison the gold distribution (green) is the inverse, so has a peak in the distribution where the silicon has its minimum. This confirms the presence of gold grain and its shape. The last distribution on the linescan is that of titanium (red). The distribution of titanium along the linescan increases and has a peak at the central position of the grain, suggesting that titanium is present within the gold grain and not on the substrate surface.

It is important to note that figure 32 is not a quantitative as K and L series signals have different cross sections.

Experimental Run 8

The temperatures to which the gold on titanium samples have been exposed to so far have all produced randomly orientated crystals. It is a result of the temperature being too high. The temperature will therefore be lowered to 400°C allowing a lower limit of the range of the break-up of the gold-titanium may be recorded.

Samples Used

Three samples will be used, all consisting of the same thickness of the gold film (20nm), two with the adhesion layer (chromium and titanium) and the third with no wetting layer present.

SEM Images

The annealing at 400°C gives some interesting results. Figure 33 shows the gold sample with titanium as the adhesion layer. This is very exciting as the gold in the figure has already dewetted into the individual gold grains but not into the randomly orientated crystals as no facets are visible and the gold has still retained its grain like shape. The gold has broken up into the individual grains only after heating for one hour at 400°C. At the same temperature the gold on chromium samples remain in flat film phase with holes just starting to appear. The differences in temperatures between the two samples and when the gold has completely broken up to form the individual grains is paramount to the different interface materials having different properties upon heating, by this weather acting as a lubrication or adhesion layer.

The percentage coverage of the gold film is 19.8% in comparison with the higher temperature annealed samples at 650° is 15.6%

In the figure a similar pattern is starting to be seen to that of the gold-chromium samples. This is the gold grains aligning in specific patterns on the substrate surface, on the gold-chromium sample the crystals aligned themselves surrounding the edge of the holes outlining the hole shape. In figure 33 a similar effect can start to be seen particularly in the highlighted region of the image, it shows the grains aligning in an almost perfect circle. The aligning of the grains to form circles is viewed across the sample and not just

in the local area. This would suggest that the earlier stage of the dewetting of the gold film is that of the hole formation.

Using the conservation of mass as the temperature is low so as to prohibit any evaporation the height of the individual grains in figure 33 can be calculated. This is done by the assumption that all the gold while in film format in SEM image has the same volume as when in individual grains (conservation of mass) then this yields an average grain height as 215nm.

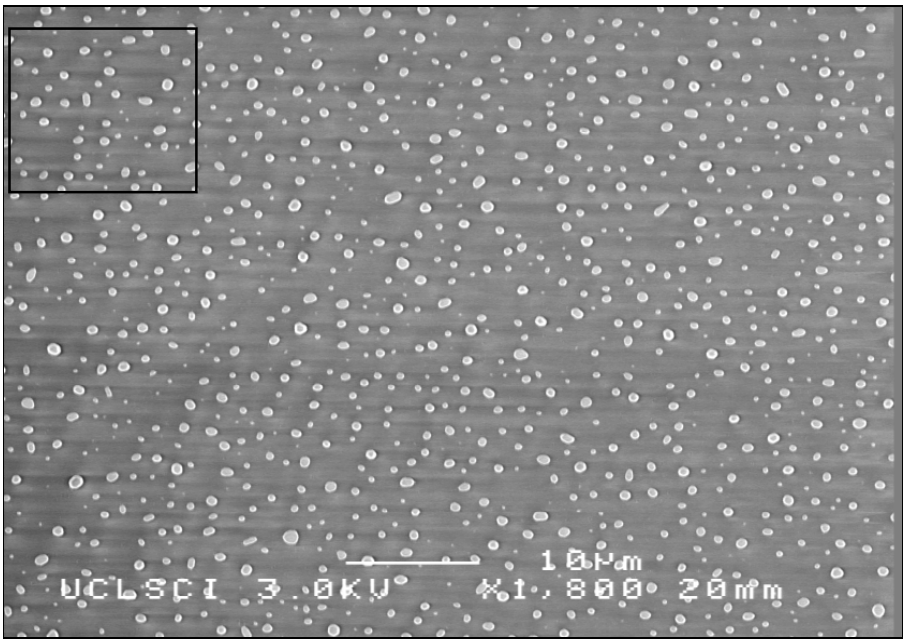

Figure 33: Gold on titanium sample after annealing to 400℃.

In comparison to this the gold-chromium sample shows a 1.88% coverage of holes in the gold film, and so a decrease in the relative stage of dewetting. The sample is largely still in gold film format (See Appendix 13), however a variety of different sized holes is visible on the sample. The presence of the different sizing of the holes is evidence of not only the hole size and number but also that the holes start to appear at various different temperatures as the film begins to weaken due to temperature increase or as time progresses.

The reason the variation in the pinholes can be seen is due to the annealing taking place at the lower temperature. At the high temperature annealing the temperature range at

which the smaller pinholes structures are visible is considerably smaller so less likely to be observed as progression into larger holes ≈5-10μm becomes more rapid.

The result at this temperature is the gold-titanium sample is comprised of individual gold grains at extremely low temperatures when current methods for crystal formation with similar samples are taken into account.
Current methods for the formation of the randomly orientated crystals comprise of the heat treatment of the sample to 1050°C for 10 hours then at 850°C for a further 8 hours, with a gas flow rate of 200sccm of nitrogen [1].

The gold samples with no adhesion layer present did not yield any useful results as it contained an abundance of contaminants, it was therefore this reason that the result was discarded.

Experimental Run 9

The results collected for the gold-chromium samples have all shown an increase in the hole area size and number. To express an accurate relationship for this more of the lower temperature samples have to be studied. It is because the lower temperature samples are still in thin film phase and the holes are complete whereas at the higher temperatures the holes can only be observed from the surrounding effect (crystals marking the hole edge). The advantages of having complete holes is that it makes for a higher accuracy in the programme analysis of the area of hole coverage (See Appendix ImageJ method) therefore no operator input for the changing of the threshold for the relative intensity is required.

Samples Used

To obtain the complete range of temperatures one final experimental run at 450°C is to be done. The samples used will be the gold-chromium and the gold with no wetting layer.

SEM Images

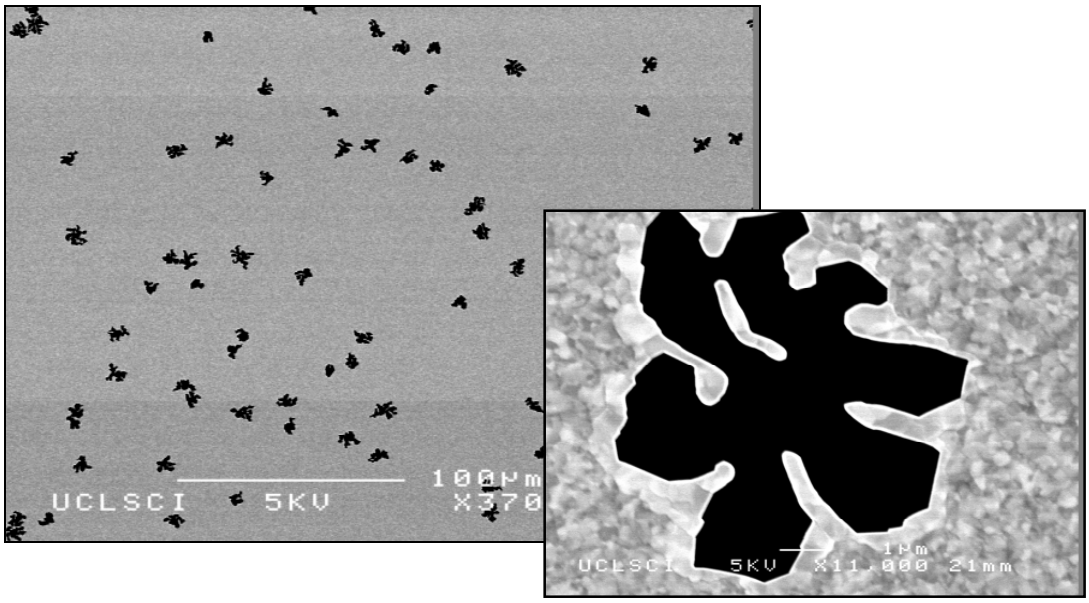

Figure 34: Gold film on substrate with no adhesion layer after heating to 450℃.
Insert: Increased magnification of hole formation.

The annealing of these samples at 450°C shows the formation of the holes on the sample with no adhesion layer present. All previous temperatures of samples with no adhesion layer have shown no hole formation. The experimental run showed the formation of the holes across the sample with some different properties to those seen before.

Figure 34 shows an increased magnification of one of the holes that is present throughout the sample. The hole is similar to that of those seen in the samples with the chromium adhesion layer. The shape of the hole viewed above is of a flower type arrangement whereas the gold-chromium samples are nearly perfect circles. The hole appears to start as a pinhole (hole through to film to the substrate layer) then grow, the growth of this hole follows in-between the rivers which create the flower like shape. The rivers which are formed from the growth of the hole are all orientated towards the original location the hole formation, upon further heat treatment these rivers would then break away from the main film creating the isolated gold islands. An example of a single river breaking away from the main film can be seen in figure 34.

A feature that can be seen is that of the surface edge lip on the gold film, it is clearly visible on the magnified image in figure 34. It shows the lip surrounding the film of the hole to a distance ~500nm from the edge of the gold. It can be viewed as the contrast and brightness were changed when the beam was focused onto the film. It then highlights the individual grains while still in film format, the grains surrounding the hole show an increase in the average grain size of the gold from ≈20nm in the bulk to be ≈200nm at the hole edge. The increase in the grain size shows the grain growth processes occurring. The lip effect seen on all previous images of the gold plates is due to the grain growth processes not from the increase in SiO_2 thickness although this may still play a small part.

The gold-chromium sample shows the same pattern of phenomenon as seen throughout all the gold-chromium samples, this being the formation of the holes and the increase in size and area with temperature (See Appendix 14).

Graph 3 shows the relationship between the percentage area of hole coverage of the sample versus temperature. This data is taken from each completed experimental run. It

appears that this forms an exponential function with the asymptote at ≈800ºC which is the temperature when the gold film completely breaks up into individual islands of the gold film, grains and crystals.

The red points on the graph are the two samples that were taken from an entirely newly created sample (See next section). It can be shown that the samples from the different wafer agree with the previous results from the first wafer.

The error on the graph is from two main sources, first the error associated with each pixel as it has no definition if the hole edge stops at the edge of a pixel or in the middle. Secondly by changing of the image to binary and altering the threshold relative intensity (See Appendix ImageJ) which is operator dependent. The largest source of error is the changing of the threshold, and intensifies in error with an increase in temperature as the gold film breaks up more, however it is difficult to obtain values, so the error on the graph below is that associated with the position of the hole with respect to the pixel.

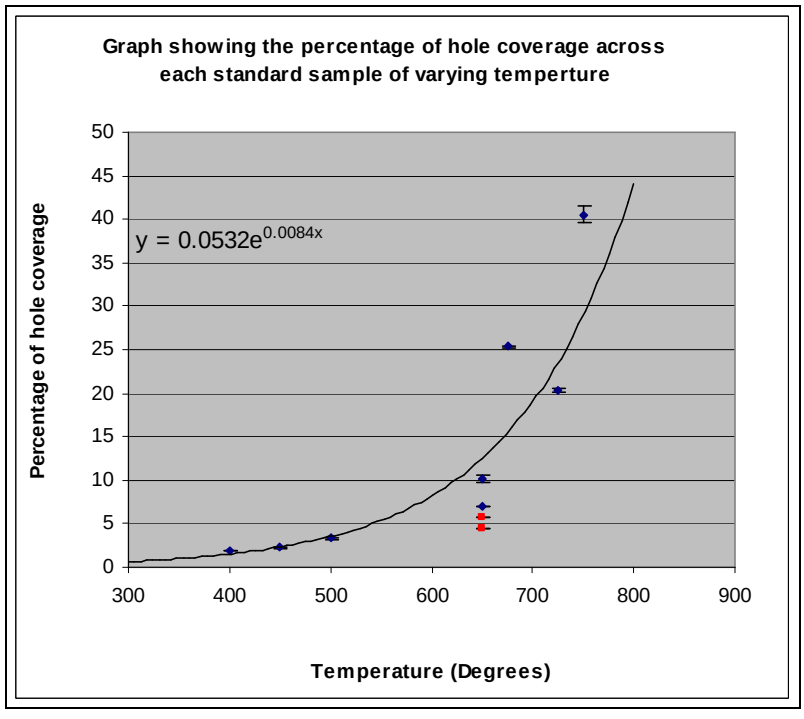

Graph 3: Graph showing the exponential relationship between temperature and the percentage area coverage of the holes.

A log graph of the graph 3 can be seen in Appendix 15 which was used to confirm the results and to predict the percentage of hole coverage before the sample was analysed.

Reproducibility

The results collected for the gold-chromium and gold-titanium samples have all come from the same wafer evaporation. To ensure the results collected are not due to some anomaly of the evaporation procedure, a second wafer was created using the same method as that previously. It will ensure consistency and agreement with previous results and confirmation that hole formation is a vital step to crystal synthesis.

The samples were evaporated with 20nm gold, 2nm chromium/titanium. The samples were annealed to 650ºC for the gold-chromium as this has been the most investigated temperature and 250°C for the gold-titanium so as to put a range on the gold break up. The annealing procedure was exactly repeated as from previous experimental runs.

Firstly the gold-titanium samples at a temperature of 250°C showed no sign whatsoever of holes/grain boundaries or any other structure on the gold surface thereby putting a lower temperature on the range at which the gold-titanium samples break up into individual grains or show any crystal synthesis. An image of the gold-titanium sample surface can be seen in Appendix 16.

Figure 35 shows the SEM image of the gold-chromium sample which was taken from a newly created evaporation to check reproducibility and was annealed to 650°C. It shows the formation of holes thereby confirming that the hole formation is a property of annealing and a part of the gold crystal synthesis process. This result shows all previous samples with the hole formation to still be valid. The image however still does not show any sign of the grain boundary formation furthering the suggestion that the structures are too small or not present.

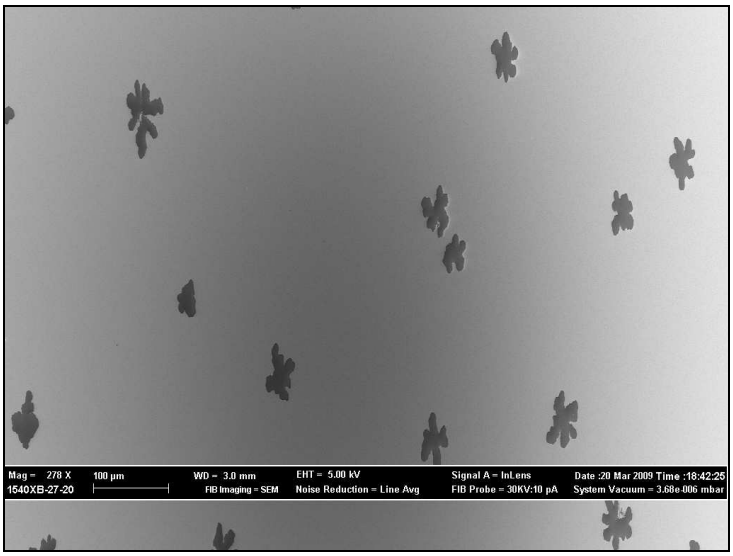

Figure 35: Image of Gold-chromium samples taken from new evaporation; annealed to 650℃.

The percentage of hole coverage of this sample is 5.7% and so agrees with the previous run.
(See Appendix 17 for gold on substrate images).

Diffraction Experiment Data

The gold-titanium samples that were annealed to a temperature of 675ºC and 400ºC were packaged in nitrogen and then sent to the Argonne laboratory in Chicago for X-Ray diffraction experiments of the samples to take place.

The results yielded that the 400ºC samples give the better diffraction pattern. This can be said as the images in figure 36 clearly show defined diffraction patterns with clear concentric rings suggestion the crystal still has some spherical shape. However the fringes that are observed are due to opposite facets on the crystal. Each image in figure 36 shows the distribution of the (111) Bragg peaks of the crystal. The images are the Fourier transform of the crystal after only having measured the intensity. The fringes that can then be used to give a size of the crystal as they correspond to the facets. The distance between fringes can be put into Braggs equation to calculate the crystal size.

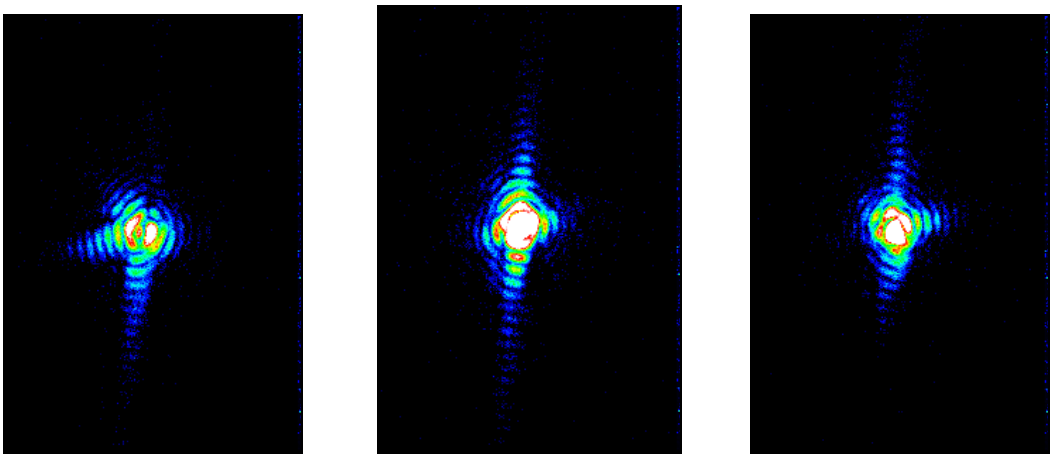

Figure 36: Diffraction images of 400ºC sample using beam of wavelength 0.139nm.

The diffraction pattern for the 675ºC did not however give such nice diffraction patterns, this can be seen in figure 37 below. The images do not give as clear defined fringes as those on the lower temperature annealed sample. This suggests that facets are not clearly defined therefore the 400ºC sample has a more crystalline structure. This was generally seen across the sample and is currently unknown why the low temperature annealing of the samples yield better defined crystals then that of the higher temperature processes.

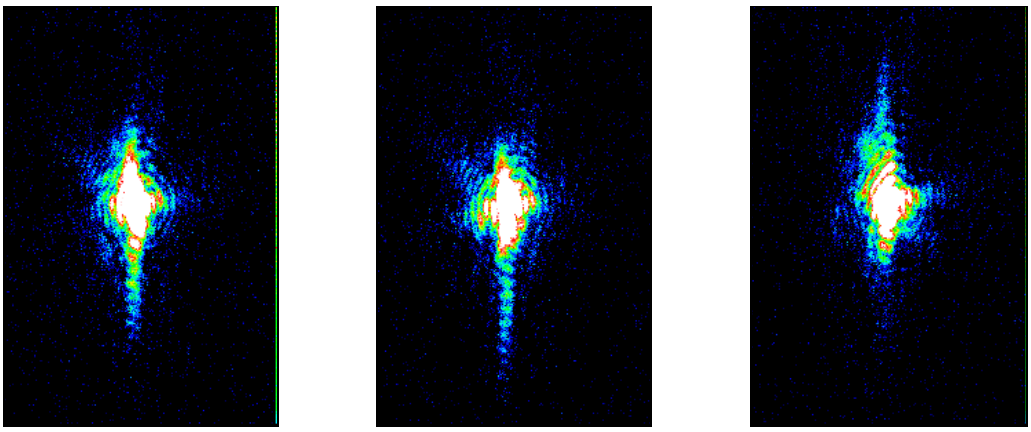

Figure 37: Diffraction pattern of 675ºC sample

Chapter 5

Conclusion

From all the data obtained from multiple experimental runs, there are a number of conclusions that can be drawn from the work carried out.

The hole formation seen throughout the samples with chromium adhesion layer is a method of gold crystal synthesis rather than grooving. The holes formed are a property of the annealing process and increase in size, area and number with an increase in temperature. The hole formation starts at low temperature with the formation of pinholes ≈<400ºC. In the temperature range of 675-725°C the gold film completely breaks up into isolated regions of gold film and individual grains for samples of gold-chromium. The grains grow into the randomly orientated crystals positioned such that the hole is visible. The holes show an exponential relationship between percentage coverage of the holes with temperature. The grains grow into the crystals before breaking apart from the isolated island then grow in size by coarsening and then start to form facets, so grains are continuing to grow throughout the crystal synthesis process.

In comparison the samples with only gold present (no adhesion layer) they indicate hole formation, but these holes only start forming in the temperature range 250°C-450°C and appear in a narrow temperature range. The shape is of such that it leads into the production of rivers from the hole. The rivers then break apart to from grains and ultimately crystals. This process is appears to be fairly uniform across each particular sample and so the polydispersity of the sample is minimised for low temperatures. The samples tend to show much clearer large grain boundaries particularly on the rivers at a range of temperatures.

The gold film samples with no intermediate layer were also the only samples to show that the lip on the edge of the gold isolated plates/islands which is due to the grains at the edge of the gold island growing in size. It is by coarsening and coalescence and so therefore increase in height as well giving rise to the lip observed.

The samples with titanium as the intermediate adhesion layer break up into the individual grains in the temperature range 250°C-400°C with facets forming on them below 650ºC.

It is not currently known as to the process of dewetting of the gold-titanium samples as upon the 400°C the sample had already broken up into uniform individual grains. However as with the gold-chromium samples it can be observed approximately every 5-10μm the grains seem to arrange themselves into a circular arrangement. This would suggest that gold-titanium samples also dewet to gold crystal synthesis via hole formation. However no breakup mechanism has been definitively observed to confirm this.

The low temperature annealed samples (400ºC) samples also yield much clearer diffraction patterns with clear fringes and facets when in comparison to the higher temperatures (650, 675ºC).

Other conclusions that can be drawn from this investigation are that only samples with an adhesion layer show a grain boundary "cobbled path" effect on the substrate. Upon experimentation with chemical analysis this structure is found to be the imprint of the adhesion layers grain structure into the silicon dioxide layer. The structure also varies in size depending on weather chromium or titanium is present on the sample surface. The titanium seems to leave a smaller grain imprint on the silicon dioxide in comparison to chromium.

The chromium adhesion layer through chemical analysis diffuses through the gold film to the surface where upon contact with ait forms Cr_2O_3, but chromium cannot be seen once the gold has broken up to individual grains suggesting the evaporation of the chromium. In comparison the titanium adhesion layer is still visible when the gold has fully dewetted, therefore the titanium either resides on the surface of the individual gold grain or interdiffused throughout the grain/crystal.

Finally the adhesion layer plays a crucial role in the dewetting of the gold film to produce randomly orientated crystals. The intermediate layers, so the titanium and chromium have very different properties. The chromium acts as an adhesion layer sticking the gold to the surface of the wafer and increasing the relative temperature of breakup. Titanium acts as a surfactant layer decreasing the temperature of the breakup of the film therefore acting as lubrication.

Future Work

Future work that this project may lead onto is varied and with huge potential. The nature of the project leads onto further work due to the increasing nanotechnology industry. Throughout the project a lot of variables were held constant thereby allowing meaningful results to be collected.
Future work directly related to the project would be to narrow the temperature range put on the gold-chromium and gold-titanium samples so a specific temperature may be found for the breakup of the film due to the hole formation in chromium samples and to find the breakup mechanism in titanium samples. To check all the results are reproducible with multiple sample evaporations from different evaporator equipment thereby eliminating any contaminations possibly present in evaporator. With multiple evaporations different thicknesses of the films can be investigated to show consistent results with 20nm films or if there is another unexpected relationship between film thickness and film breakup.

Throughout this project the coarsening and coalescence of the grains to crystals has not accurately been observed so annealing samples at frequent and regular temperature intervals would enable an accurate model of the grain growth to crystals to be formed thereby allowing for a rate of the total growth processes to be calculated.

This project only imaged the samples with an SEM, an alternative measurement which would give resolution to the nanometre scale would be using an Atomic Force Microscope (AFM). It would have the potential to give much more accurate resolution on the shape of the grains and if their are grain boundaries that cannot be imaged under SEM due to the electron beam induced deposition. It would still only give data from the mid point on each grain as it works by dragging a point across the surface and measuring the change.

Other possible investigations may look into the variables held constant for this project. This could be such as the adhesion layer. The adhesion layers used were Titanium and Chromium but this could be extended to Aluminium, Nickel and Tungsten all of which have been used in other investigations in the same context as chromium and titanium as for this project but not studied in detail for low temperature annealing. It would yield

useful information on the effect each material has at the same applied temperature. Gas flow combinations and annealing under vacuum can also be investigated.

One other aspect of future work would be to investigate the further uses of gold-titanium low temperature crystals in other aspects of nanoscience.

Other areas of nanoscience that would prove useful would be the dewetting properties of patterned samples of gold. This would be in accordance with nanotechnology industry and the production of sensors at the nanoscale in the future.

Appendices

Appendix 1

London Centre for Nanotechnology and laboratory training

-London Centre for Nanotechnology Health and safety induction.

-Cleanroom access training.

-Bell jar and electron beam evaporator training.

-Furnace tube exchange and operation.

-Scanning Electron Microscope training.

-London centre for Nanotechnology

-Institute of archaeology

Lab supervisors: Moyu Watari, Steven Leake, Marcus Newton, Loren Bietra, khashayar Ghaffarzadeh, Kevin Reeves (Institute of Archeology).

For each training and most laboratory sessions an Inter-Departmental Transfer must be completed before each associated session can take place.

The table below shows the samples that were used for the duration of this project, the temperature they were annealed at and the SEM that was used for the analysis of the samples.

	Annealing temperature (°C)								
Samples	250	300	400	450	500	650	675	725	750
Gold+Chromium	Yes	Yes	Yes	Yes	Yes	Yes	Yes	Yes	Yes
Ramped Gold	No	Yes	No	No	No	Yes	No	No	No
Gold+Titanium	Yes	No	Yes	No	No	Yes	Yes	No	No
Gold	Yes	No	No	Yes	No	Yes	Yes	No	No
Patterned Gold	No	No	No	No	No	No	No	Yes	No
SEM Location image	LCN	LCN	-	-	LCN	LCN	LCN	LCN	LCN
taken	-	-	ARCH	ARCH	-	ARCH	-	-	ARCH

LCN = London Centre for Nanotechnology
ARCH = Institute of Archaeology

Appendix 2

For the purging of the furnace with nitrogen before annealing, the following equation is used for minimum purging time.

$$C_n = C_0 e^{-V/St}$$

C_n = Current concentration of dust particles and anomalies
C_0 = Initial concentration of dust particles and anomalies
V = Volume of furnace tube (2748sccm)
S = Flow rate of gas (Nitrogen 500sccm)
t = Time

The time therefore required to be below 25% of the initial value will take ~6.5 minutes. The time is extended greater than this before annealing to ensure clean conditions.

Appendix 3

The following images are all from the same sample, which is that of the 650°C gold ramped sample. The range, magnification and number of images were for the variety of the structures observed was replicated for each different sample at each temperature.

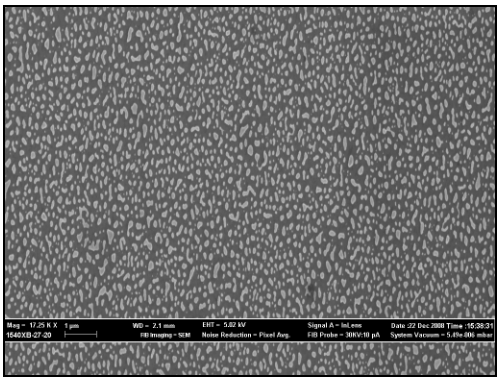

Image 1: Location 1 on Figure 14

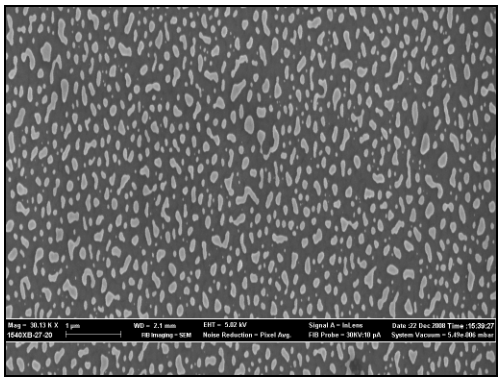

Image 2: Location 2 on Figure 1

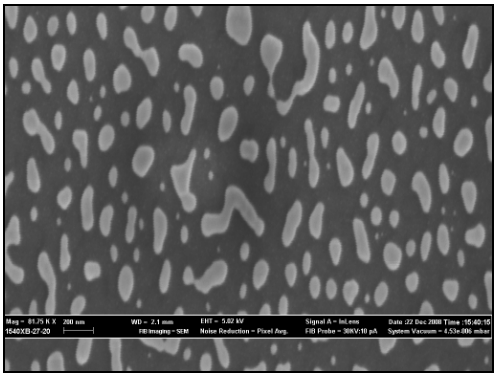

Image 3: Location 3 on Figure 14

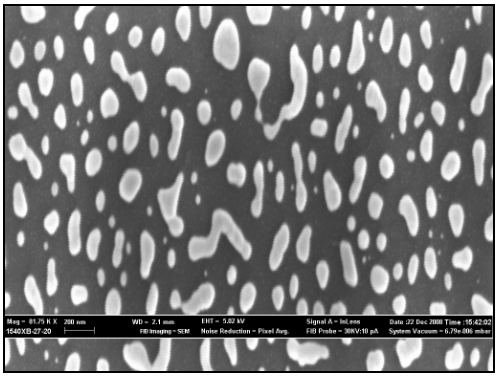

Image 4: Location 4 on Figure 14

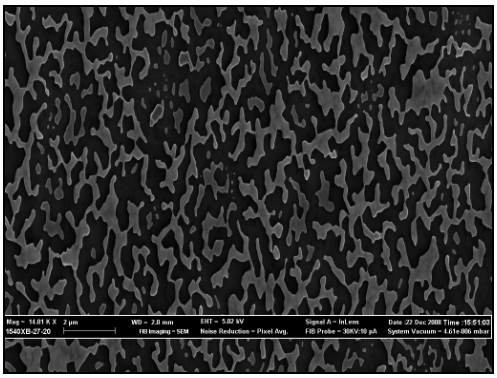

Image 5: Location 5 on Figure 14

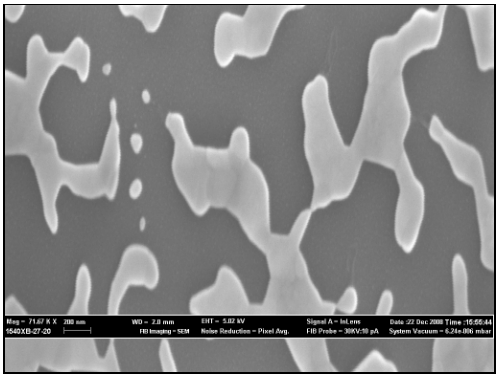

Image 6: Location 6 on Figure 14

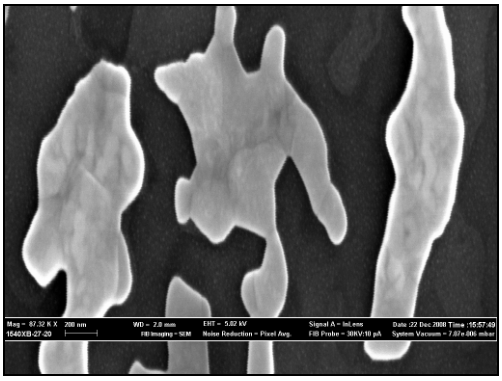

Image 7: Location 7 on Figure 14

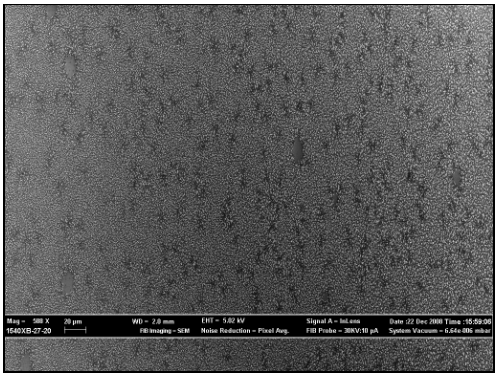

Image 8: Location 8 on Figure 14

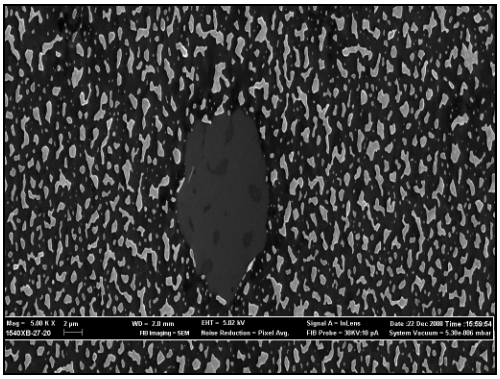

Image 9: Location 9 on Figure 14

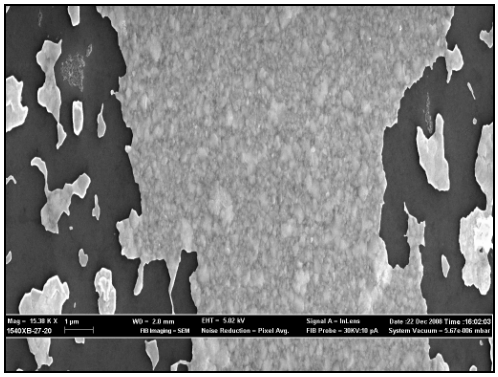

Image 10: Location 10 on Figure 14

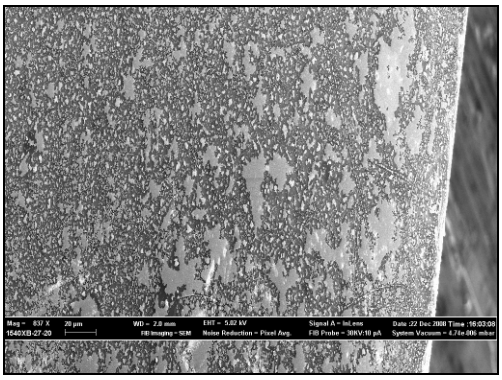

Image 11: Location 11 on Figure 14

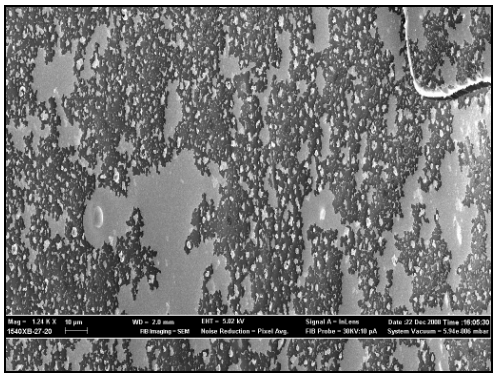

Image 12: Location 12 on Figure 14

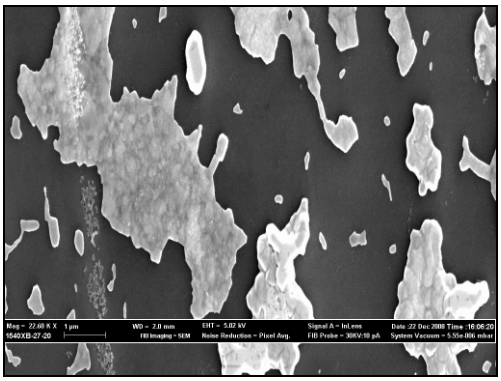

Image 13: Location 13 on Figure 14

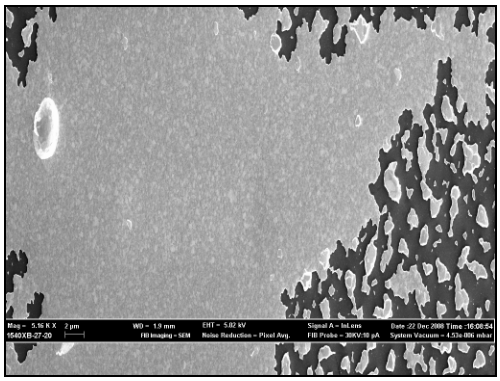

Image 14: Location 14 on Figure 14

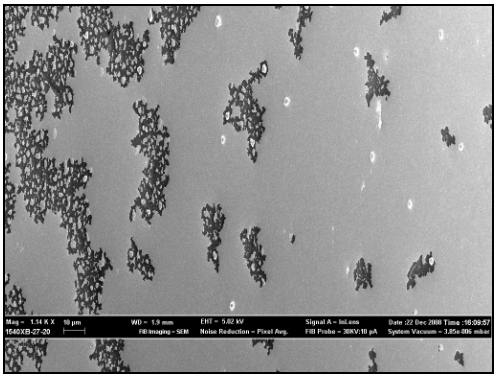

Image 15: Location 15 on Figure 14

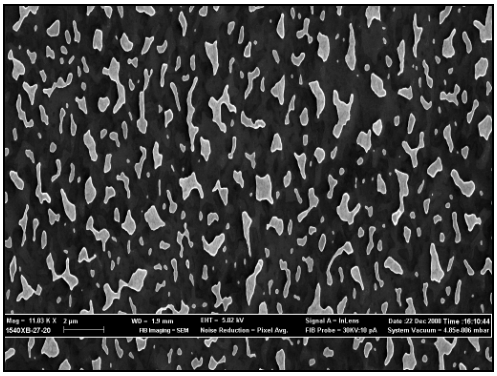

Image 16: Location 16 on Figure 14

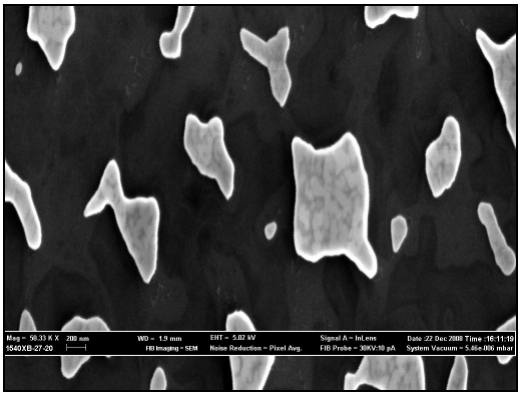

Image 17: Location 17 on Figure 14

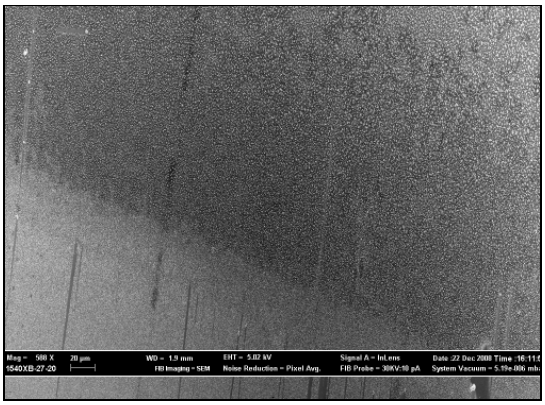

Image 18: Location 18 on Figure 14

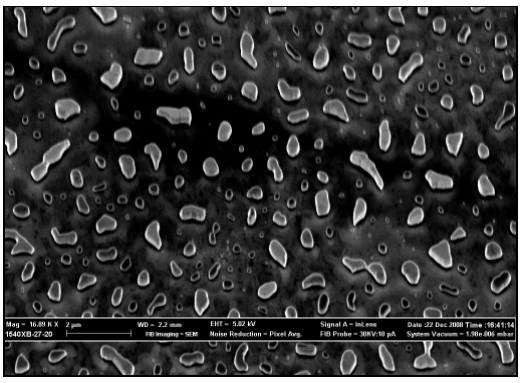

Image 19: Location 19 on Figure 14

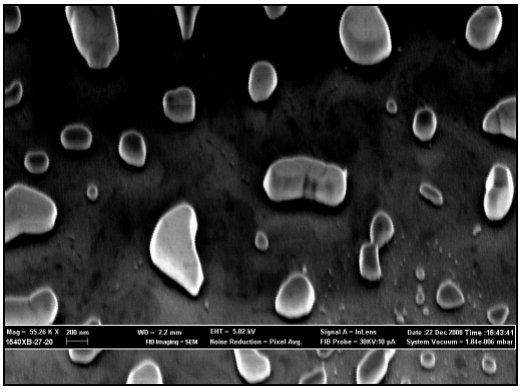

Image 20: Location 20 on Figure 14

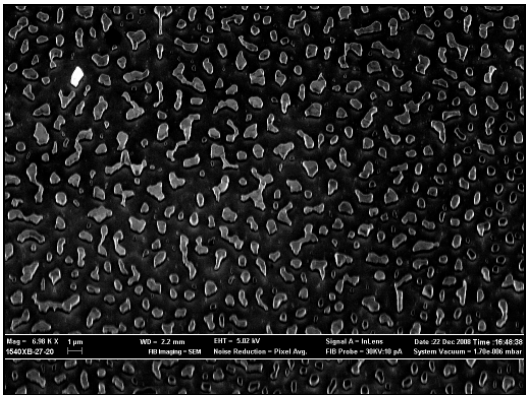

Image 21: Location 21 on Figure 14

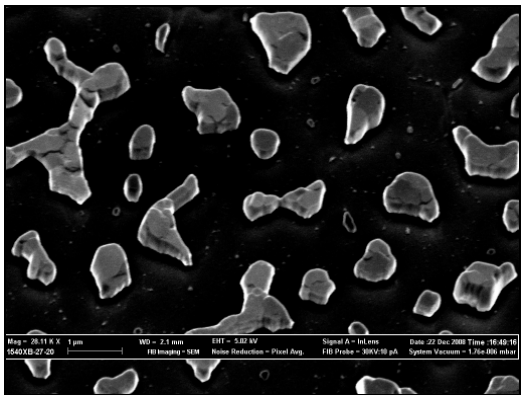

Image 22: Location 22 on Figure 14

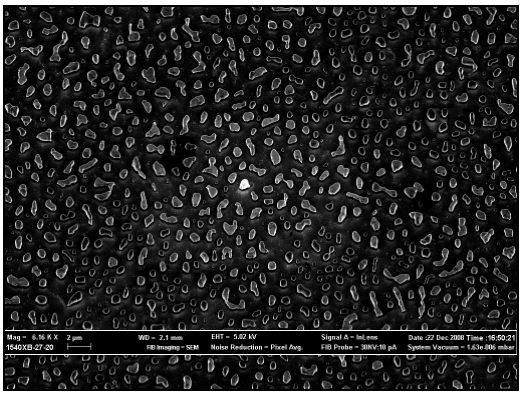

Image 23: Location 23 on Figure 14

ImageJ

Version 1.41

ImageJ is an image analysis package which has multiple functions relevant to the analysis of this project.

The benefit of using this package is that usual functions such as sharpening and enhancing the image as well changing the contrast and brightness of the image are all available.

There are more complex functions which were of great importance for the duration of the project, this would be such as calculating the area of the hole coverage of the sample and the size of the individual gold grains. The final function that was used throughout the project is that of plotting the 3D representation of the gold grains.

For the use of these functions to achieve the desired results other settings and functions need to be changed.

An example of this would be the methodology of area analysis of the holes.

This is achieved through a number of stages, firstly the conversion of the required image to an 8-bit image. Once converted the relative intensity needs to be modified, as the SEM works by seeing a difference in structures due to the change in the contrast. This means that different structures on the image may have similar contrasts so the programme has trouble differentiating between the two. The difficulty in distinguishing between the contrasts then becomes more apparent with the next stage which is converting to a binary image, which is necessary for the particle analysis.

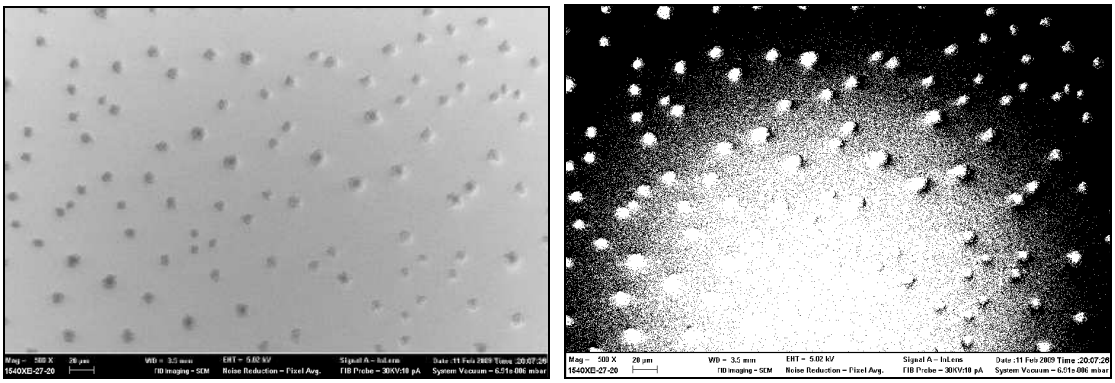

The two images above show the original greyscale image collected from the SEM on the left, and the original image directly converted to binary without altering the threshold for the relative intensity is shown on the right. The image shows that without filtering out any of the relative intensities a lot of the information held in the image is lost.

The changing of the threshold is because each pixel records the relative intensity observed and so a distribution of relative intensity with respect to number of pixels may be created. This is shown in the image below where the solid black vertical line is the new cut off for the relative intensities. Any above this value in the image will be scaled to white.

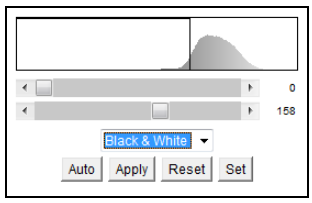

With relative intensity threshold now changed the binary function can now be applied. The image below shows now the benefit of this process as much of the image quality of the holes has been retained.

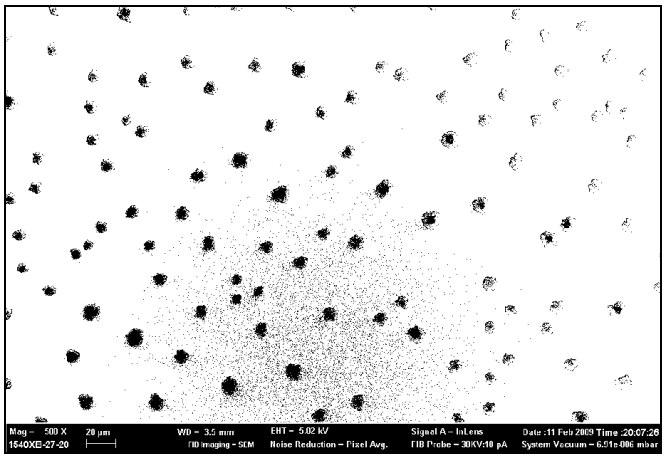

The analysing particle function can now be used. This function takes the image and records the area and size of all particles with the circularity defined by the operator. This therefore can give the area of every particle/hole in the image therefore enabling the calculation of percentage coverage of gold/holes.

The three dimensional images created using this programme use both the X and the Y coordinate as normal then use the relative intensity as the third dimension. The disadvantage in this is that only the information from the grains equivalent equator is observed as the images are taken perpendicular to the surface of the sample.

Most of the programme was explored for possible uses related to the images collected from the SEM, however only the functions described above were used for the majority of the time for the project.

Appendix 4

The graph below shows the grain size distribution for experimental run 1 at a temperature of 650°C. The data was taken with the longest orientation of the grain being the grain size. The distribution from this data set however does not give such a clean result, the conclusion from this is that as the image is skewed in one dimension thereby giving an inaccurate grain size due to the SEM.

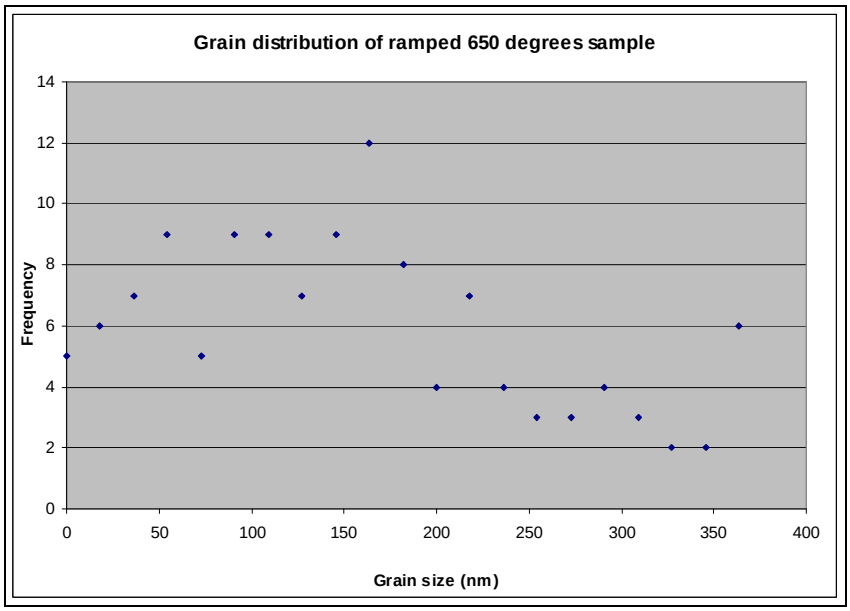

Appendix 5

The images shown below are both from the same sample being 650°C ramped sample. The differences arising from the SEM used to capture the image. The left hand image was captured using the SEM from the Institute of Archaeology and the right image from the London Centre for Nanotechnology. What can be observed is that there is a difference in the average shape of the gold grains under observation. Those imaged using the SEM from the institute of archaeology are spherical in shape as expected whereas those from the London centre for Nanotechnology all appear stretched and the image seems skewed. This would most likely be due to the conductive tape not being flat.

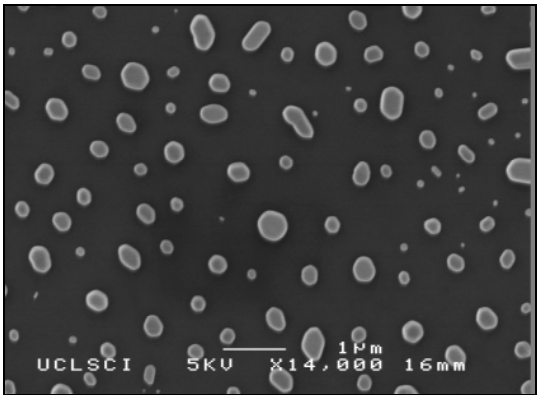

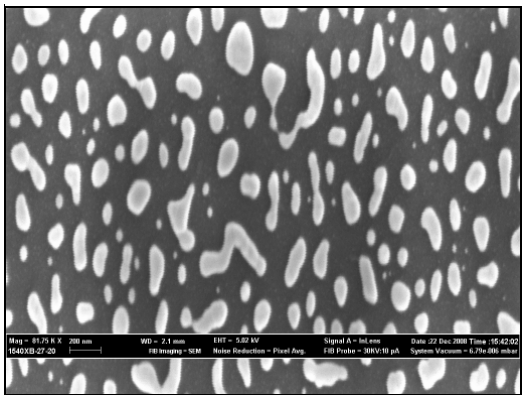

Institute of Archeology *London Centre for Nanotechnology*

Appendix 6

The images below are a selection of sequential images taken from the 300ºC Ramped sample with no adhesion layer present.

The images show the thickest of end of the sample being the image on the left, and hence the thinnest gold coverage is the image on the right.

It can be seen from the images that for the majority of the gold film on the sample is still in flat film with only the starting formation of holes visible but as this is at the thinnest end of the sample and the thickness where the image was taken is unknown it is of little use.

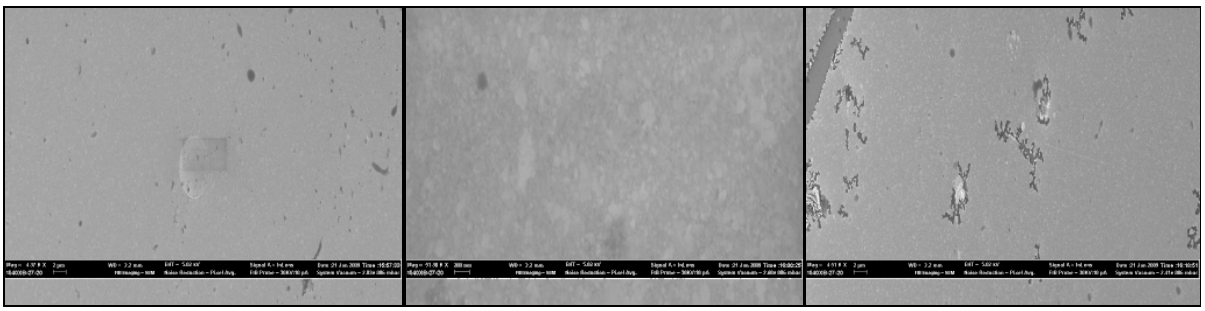

Appendix 7

The image below is of the 0°C sample. Although the image shows a hole this would be an irregularity in the oxide layer and nothing with the annealing process. It was imaged as an area which the SEM could then be focused onto.

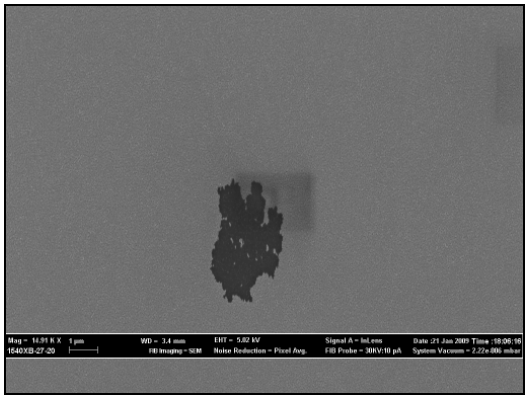

Appendix 8

The image below is that of the 750°C sample at the edge of a hole. The gold film and the individual grains can be seen in the image as well as the grain boundary pattern of random shape imprinted onto the silicon substrate from the adhesion layer.

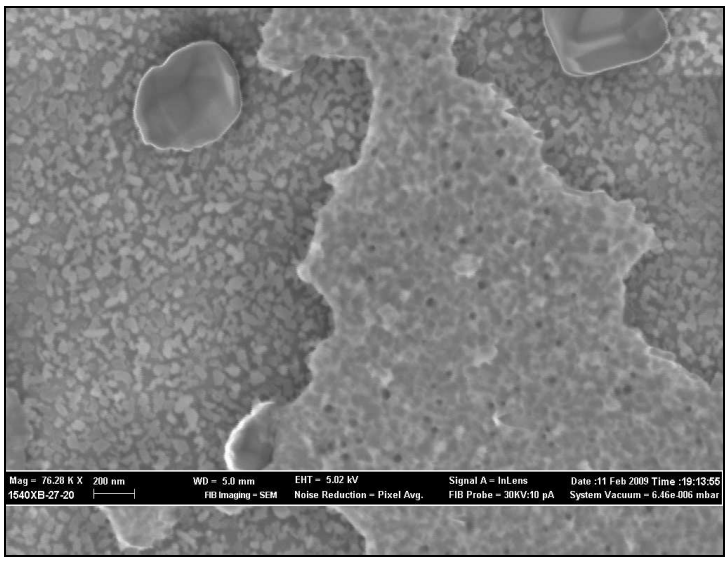

Appendix 9

The spectrum below is of a single gold grain of which a compositional image has been acquired. The spectrum shows the gold peaks as well as those for silicon, oxygen and carbon due to the excitation of the atoms in the surrounding area and reaction with the air.

The X-ray spectrum analysis was collected using the Inca programme whereas the image collection uses Semafore.

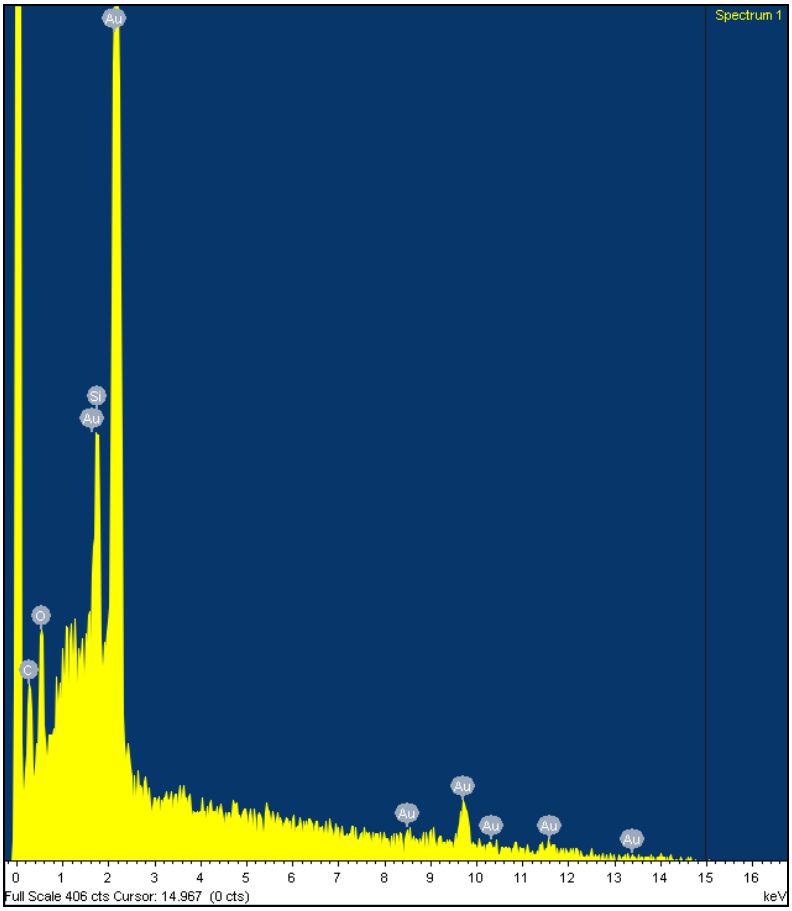

Appendix 10

The 725°C sample shown below was assumed to be an anomalous result. The result was omitted from the investigation as no film or crystal grain properties were observed.
The image shows what was the gold film, has coarsened and coalescence to much larger islands of gold. No grains or crystals can be observed.
The grain boundary pattern however can be observed on the substrate surface throughout the sample.

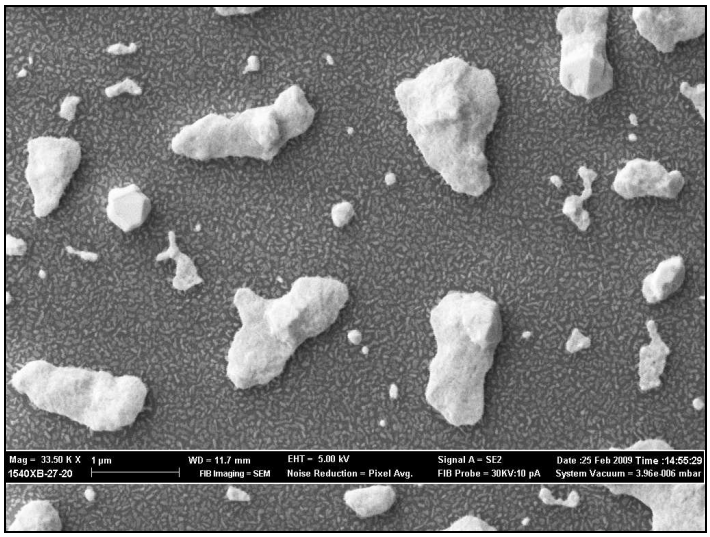

Appendix 11

A Patterned sample was also put through the same conditions as that of the standard gold-chromium sample at 725°C. The sample comprises of three different shapes which have been created by e-beam lithography. The different patterns consist of Rectangular, Triangle and Rhombus shapes and with each of them are three different associated areas.
The three different areas of the three shapes are as follows: - 0.49µm, 0.36 µm, 0.25 µm.

The three SEM images that are shown below is of the three different shapes all of which have the 0.36µm area and are pre-annealing images, so after the e-beam lithography.

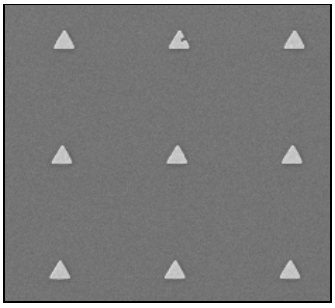

Triangular: 0.36μm

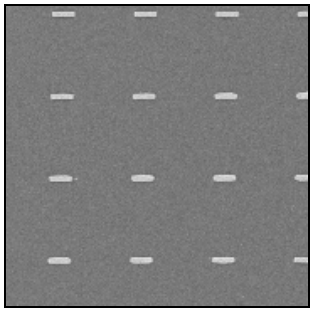

Rectangular: 0.36μm

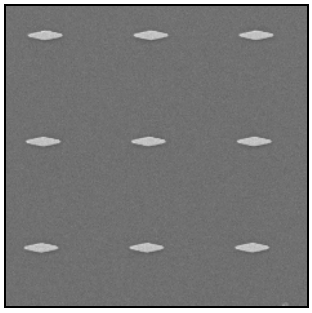

Rhombus: 0.36μm

Only the 0.36 μm areas are shown below and are all post annealing SEM images.

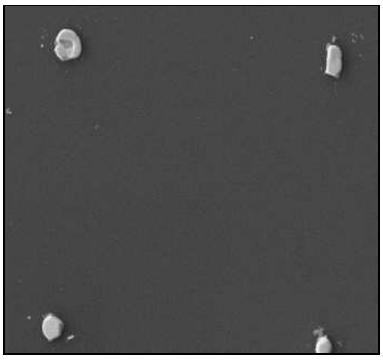

Triangular: 0.36μm

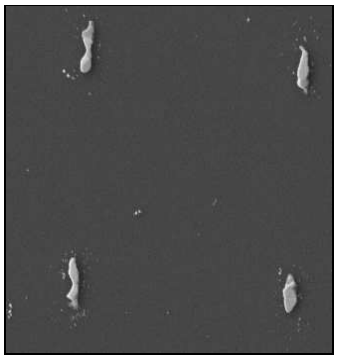

Rectangular: 0.36μm

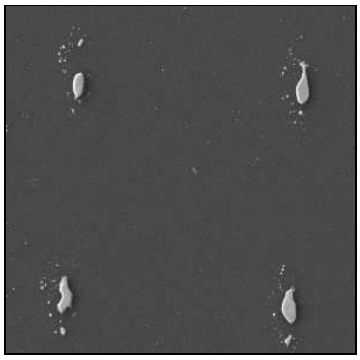

Rhombus: 0.36μm

Appendix 12

The image below is an increased magnification of the gold-chromium sample after being annealed to 675°C. The image of the edge of one of the holes so the gold film can be seen as well as the grain boundary effect seen on the substrate itself.

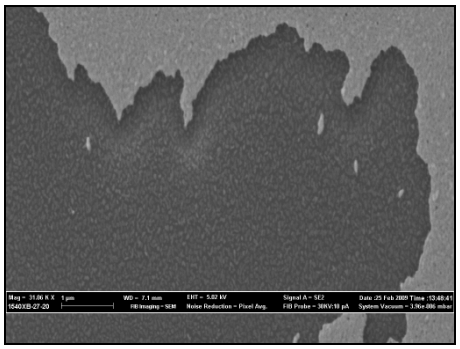

Appendix 13

The figure below is of gold on chromium sample after annealing to 400°C. It shows the holes present across the sample and the difference in the sizes of the holes as they start to form.

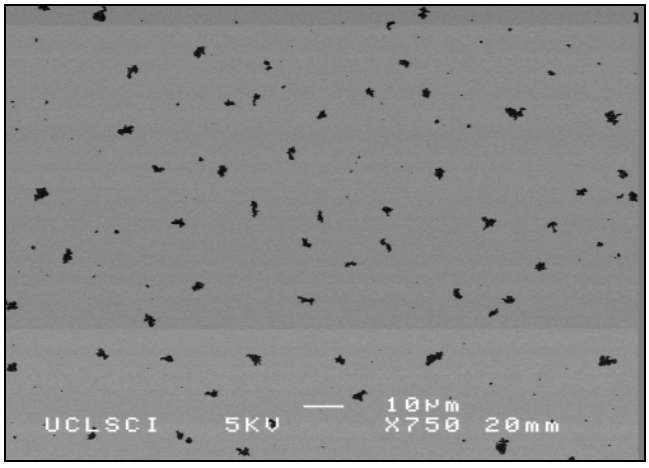

Appendix 14

Below is the SEM image of the gold-chromium sample after annealing to a temperature of 450ºC. It clearly shows the variation in the hole formation size from the pinholes which are under 1µm in size to the holes of order size seen at the higher temperatures (5-8µm).

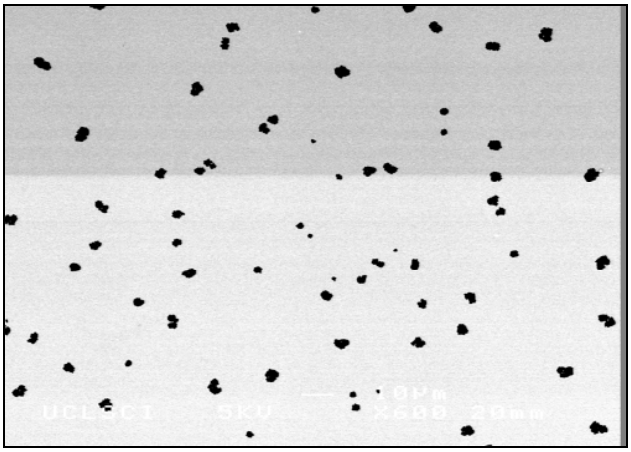

Appendix 15

Below is a graph showing the log of the percentage of hole coverage plotted against temperature for the gold-chromium samples. This graph again shows the two red points which is the data taken from the samples from the second evaporation. This graph can then be used to predict the percentage area of the hole coverage.

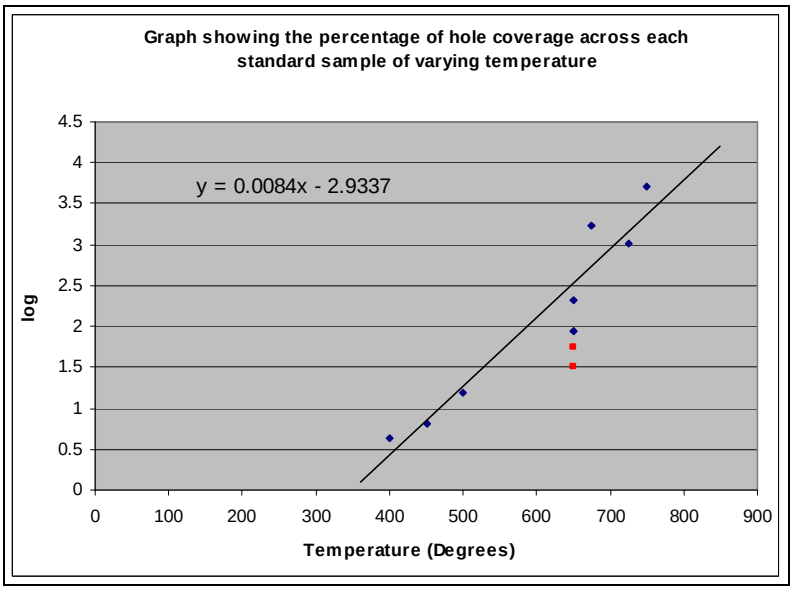

Appendix 16

The SEM image below shows the gold-titanium sample after having been annealed to a temperature of 250ºC. It can clearly be seen that there is no structures on the surface and this is observed across the sample. The individual grains can just be seen but as they are of size 20nm which is the starting size of the grains, so no coarsening of coalescence process have begun.

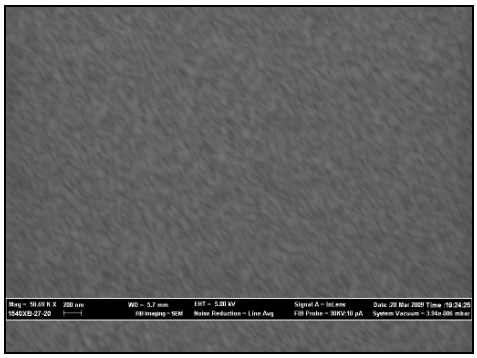

Appendix 17

The image below shows the gold (no adhesion layer sample) after being heated to a temperature of 650°C. What is most interesting about the image is the way the gold has formed a lot of little squares all in the same orientation. This is suggested by the gold in contact with the silicon and sitting in the cubic crystal structure therefore retaining its shape across the sample.

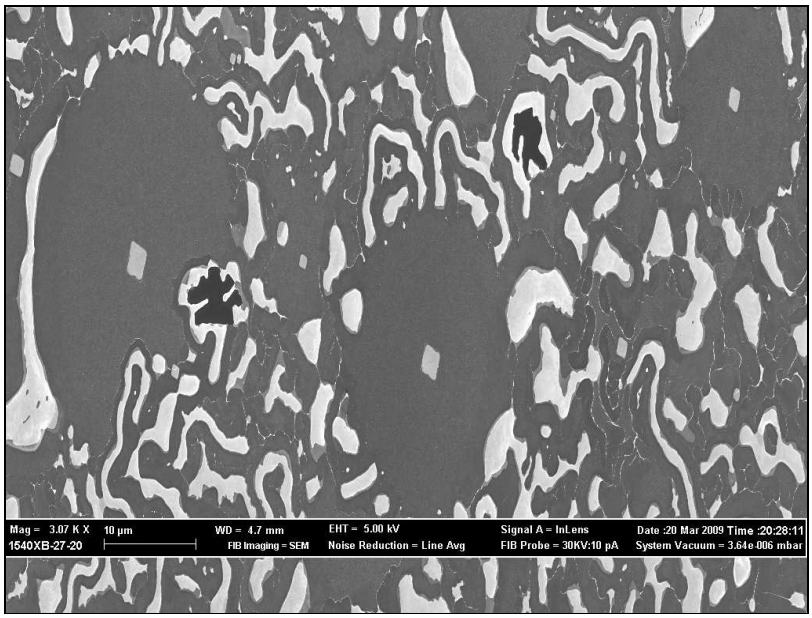

References

[1] *Microscopy of Gold Microcrystal's by Coherent X-Ray Diffractive Imaging*: Garth J. Williams: (2004): University of Illinois.

[2] *The Effect of Pressure on Grain Growth and Boundary Mobility*: H Hahn and H Gleiter: (1979): University of Saarbrücken Germany.

[3] *Microelectronic Materials: Graduate Student Series in Materials Science and Engineering*: C. Grovenor: Page 224.

[4] *Effects of Diffusion on Interfacial Fracture of Gold-Chromium Hybrid Microcircuit Films*: N.R. Moody, D.P. Adams, D. Medlin, T. Headley, N. Yang, A. Volinsky: (2003): Sandia National Laboratories, Livermore, (U.S.A); Sandia National Laboratories, Albuquerque, (U.S.A).

[5] *Annealing Effects on Interfacial Fracture of Gold-Chromium Films in Hybrid Microcircuits*: N. R. Moody, D. P. Adams, A. A. Volinsky, M. D. Kriese, W. W. Gerberich: (2000): Sandia National Laboratories, Livermore; University of Minnesota, Minneapolis (U.S.A).

[6] *Effect of Chromium–Gold and Titanium–Titanium Nitride–Platinum–Gold Metallization on Wire/Ribbon Bondability*: Jianbiao Pan, Robert M. Pafchek, Frank F. Judd, Jason B. Baxter: (2006).

[7] *Grain Boundary Diffusion Effects in Films of Gold on Chromium*: P.S. Kenrick: Nature Vol 217 March 30th (1968).

[8] *Materials Science of Thin Films*: Second Edition Deposition and Structure: Milton Ohring: Page 646.

[9] *Grain Coarsening and Gas Bubbles in Annealed Gold Films*: R. Andrew, Viktor Krasevec: (1975): Department of Electrical Engineering, University of Salford, Lancashire; Institut Jozef Stefan, Ljubljana, Yugoslavia.

[10] *Structure Evolution During Processing of Polycrystalline Films*: C.V. Thompson: (2000): Massachusetts Institute of Technology.

[11] *The Effect of Thermal Grooving on Grain Boundary Motion*: W.W. Mullins: (1958).

[12] *Grain Boundary Groove Evolutions by Surface Self-Diffusion on a Plane and Wire*: Vu Thien Binh, M Chaudier, J.C Couturier, R Uzan, M Drechsler: (1976): Department de physique des Materiaux, Universite Claude Bernard Lyon I, France.

[13] *Grooving at Grain Boundaries in Thin Films*: P.J. Goodhew, D.A. Smith: (1982): I.B.M. Thomas J. Watson Research Center Yorktown Heights, N.Y. (U.S.A).

[14] *Thermal Grooving at Migrating Grain Boundaries*: D.J. Allen: (1982): Marchwood Engineering Laboratories Southampton.

[15] Molecular *Dynamics Analysis of Grain-Boundary Grooving in Thin-Film Interconnects for ULSIs*: Tomio Iwasaki, Hideo Miura: Mechanical Engineering Research Laboratory, Hitachi, Japan.

[16] *Geometric Origin of Hexagonal Close Packing at a Grain Boundary in Gold*: G. Lucadamo and D. L. Medlin: (2003): Department of Thin Film and Interface Science, Sandia National Laboratories (U.S.A.).

[17] *Diffusion Processes in Advanced Technological Materials*: Dīvāndar Guptā: (2005) Illustrated Edition.

[18] *Heat- and Electron-Beam-Induced Transport of Gold Particles into Silicon Oxide and Silicon Studied by In Situ High-Resolution Transmission Electron Microscopy*:

Johannes Biskupek, Ute Kaiser, Fritz Falk: (2008): Electron Microscopy Group of Materials Science, University of Ulm, Germany; Institute of Photonic Technologies, Jena, Germany.

[19] *Thermal Transport Properties of Gold-Covered Thin-Film Silicon Dioxide*: Mihai G. Burzo, Pavel L. Komarov, Peter E. Raad: (2003).

[20] *Microsystem Engineering of Lab-on-a-chip Devices*: Oliver Geschke, Henning Klank, Pieter Telleman: (2006): Page 139

[21] *Relations between the Parameters of Grain-Boundary Diffusion of Zinc in Aluminum*: A.N. Aleshin: (2005): Baikov Institute of Metallurgy and Materials Science, Russian Academy of Sciences, Russia.

[22] *Characterization of Thin Titanium Oxide Adhesion Layers on Gold*: Resistivity, Morphology, and Composition: K.W. Vogt, P.A. Kohl, W.B. Carter, R.A. Bell, L.A. Bottomley: (1993): Georgia Institute of Technology, Atlanta, (U.S.A).

[23] *Spectroscopic Ellipsometry on Gold Clusters Embedded in a Si(111) Surface*: K. Mümmler, P. Wiβmann: (1998): Institute of Physical and Theoretical Chemistry of the University of Erlangen-Nürnberg, Germany.

[24] *Electronic Materials Handbook Volume 1*: Merrill L. Minges: (1989): Page 214

[25] www.ami.ac.uk/courses/topics/0203_dbm/index.html - Eutectic bond phase diagram.

[26] *Thin Film Technology Handbook*: Aicha Elshabini-Riad, Fred D Barlow III: International Society of Hybrid Microelectronics: Section 1.3.2

[27] *Synthesis of Nanoscale Structures in Single Crystal Silicon Carbide by Electron Beam Lithography*: Jay A. Bieber, Stephen E. Saddow, Wilfrido A. Moreno: (2004):

Nanomaterials and Nanomanufacturing Research Center, Department of Electrical Engineering University of South Florida, Florida.

[28] *Grain Boundary Migration in Metals*: G. Gottstein, Lazar, Simkhovich Shvindlerman: 1999: page 22, 72, 237.

[29] *Electron Beam-Induced Sample Contamination in the SEM*: A.E. Vladar, M.T. Postek: (2005): National Institute of Standards and Technology.

[30] www.siliconcert.com/sem.htm

[31] www.webelements.com

Background reading

Vacuum-Deposited Gold Films I. Factors Affecting the Film Morphology: Yuval Golan, Lev Margulis, Israel Rubinstein: (1991): Department of Materials und Interfaces, The Weizmann Institute of Science, Israel.

The Origin of Faceting of Ultraflat Gold Films Epitaxially Grown on Mica: Bjorn Lussem, Silvia Karthauser, Hans Haselier, Rainer Waser: (2005): Institut für Festkörperforschung and CNI, Center for Nanoelectronic Systems for Information Technology, Germany.

Facile Route to Ultraflat SAM-Protected Gold Surfaces by "Amphiphile Splitting": Pooja Gupta, Katja Loos, Alexander Korniakov, Chiara Spagnoli, Mary Cowman, Abraham Ulman: (2004).

Effect of Growth Conditions on Formation of Grain Boundaries in Epitaxial Silicon layers: G. S. Konstantinova, V. N. Lozovski: (2000): Ï.Novocherkassk State Technical University, Russia.

Grain Boundary Self-Diffusion in Evaporated Gold Films at Low Temperatures: D. Gupta, K. W. Asai: (1974): IBM Thomas J. Watson Research Center, Yorktown Heights, N. Y. (U.S.A.).

Grain Growth and Thermal Stability of Silver Thin Films: A.R. Shugurov, V. Panin, B.A Loginov: (2005): Institute of Strength Physics and Materials Tomsk State University, Russia; School of Materials Science and Engineering University of Ulsan, Korea; Alikhanov Institute for Theoretical and Experimental Physics, Moscow, Russia.

The Effect of Roughness on the T_3-Dewetting of Molecular Hydrogen: Jorg Angrik, Masoud Sohaili, Jurgen Klier, Paul Leiderer: (2003): University of Konstanz, Germany.

Dewetting Modes of Thin Metallic Films; Nucleation of Holes and Spinodal Dewetting: J.Bischof, D.Scherer, S.Herminghaus, P.Leiderer: (1996): University of Konstanz, Germany.

Effects of Grain Boundary Structure on Diffusion Along [001] Tilt Boundaries in the Au/Ag System: Quing Ma: (1991): Massachusetts Institute of Technology.

www.utilisegold.com/uses_applications/nanotechnology/ - Utilisegold. The World of gold science and nanotechnology.